Electronic Supplementary Material (ESI) for Physical Chemistry Chemical Physics.

Supporting Information to Thermodynamics of Supercritical Carbon Dioxide Mixtures Across the Widom Line

Denis Saric, Gabriela Guevara-Carrion, Jadran Vrabec
Thermodynamics and Process Engineering, Technical University of Berlin
Ernst-Reuter-Platz 1, 10587 Berlin, Germany

October 24, 2022

Technical details

The simulations in the NpT ensemble to determine the density were equilibrated for $3 \cdot 10^4$ time steps and followed by a production run of $2 \cdot 10^6$ steps. The simulations in the NVT ensemble were equilibrated for $5 \cdot 10^5$ time steps and followed by a production run of $20 \cdot 10^6$ to $24 \cdot 10^6$ steps.

A fifth-order Gear predictor-corrector scheme with an integration time step of 0.994 fs was used to solve Newton's equations of motion. The velocity scaling algorithm was employed to control the temperature. The pressure was kept constant by the Andersen barostat[1] with a piston mass of $2.2 \cdot 10^9$ kg m^{-4}. The cubic simulation volume with periodic boundary conditions contained 5000 molecules throughout. The cut-off radius was set to 21 Å. Lennard-Jones long range interactions were considered analytically employing angle averaging[2] and the reaction field method with conducting boundary conditions ($\epsilon_{\mathrm{RF}} = 1$) was used for the dipolar interactions.

Correlation functions were calculated from an average of $4 \cdot 10^5$ independent time origins and a sampling length of 40 ps throughout. This extensive length of the autocorrelation functions was chosen to avoid long-time tail corrections. The separation between the time origins was chosen such that all correlation functions achieved time independence and decayed at least to 1/e of their normalized value. Statistical uncertainties were estimated by the block averaging technique of Flyvberg and Petersen[3]. Uncertainties of the derived thermodynamic properties were estimated by the error propagation law.

Average relative deviation

In order to quantify the deviations between simulation and empirical data for a given mixture, the average relative deviation (ARD) was calculated by

$$\mathrm{ARD} = \frac{1}{n} \sum_{i=1}^{n} \frac{|z_{\mathrm{sim}} - z_{\mathrm{emp}}|}{z_{\mathrm{emp}}}, \tag{S1}$$

where n is the number of data points studied, z_{sim} and z_{emp} are the thermodynamic quantities calculated from simulation and empirical data, respectively.

Molecular models and validation

Table S1: Binary interaction parameter ξ for the seven binary CO_2 mixtures considered in this work. The parameters were fitted to VLE data with a procedure described in preceding work[4]. The parameters of the employed force fields are listed in the MolMod database[5].

Mixture	ξ
CO_2 + hydrogen	1
CO_2 + methane	0.974
CO_2 + ethane	0.955
CO_2 + isobutane	0.985
CO_2 + benzene	0.995
CO_2 + toluene	0.96
CO_2 + naphthalene	1

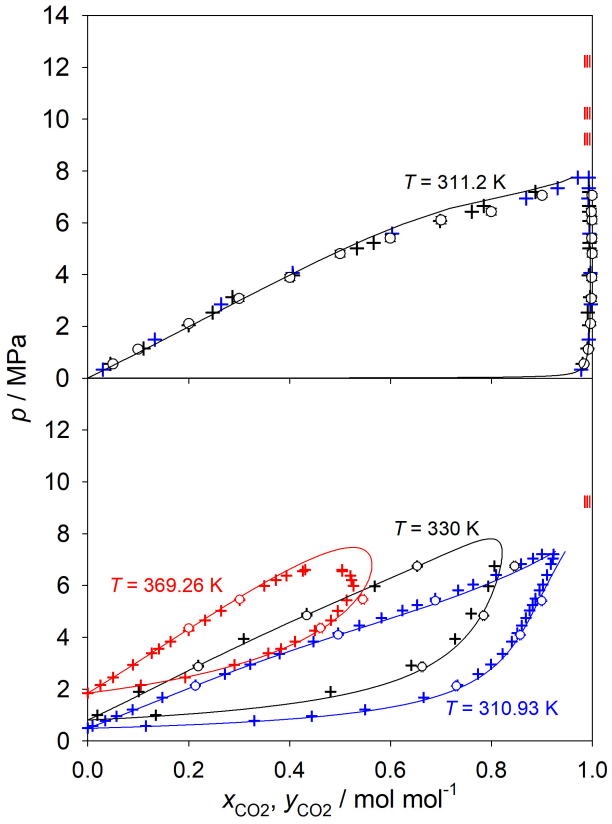

Figure S1: Vapor-liquid equilibria of CO_2 mixtures with isobutane (bottom) or toluene (top). Solid lines for CO_2 + isobutane denote data from the GERG-2008 EOS[6] and for CO_2 + toluene they denote data from the Peng-Robinson EOS (k_{ij} = 0.108)[7]. Crosses represent experimental data for CO_2 + isobutane[8] and for CO_2 + toluene[9,10], whereas circles depict molecular simulation results. Red vertical marks on the very right stand for the supercritical states of interest.

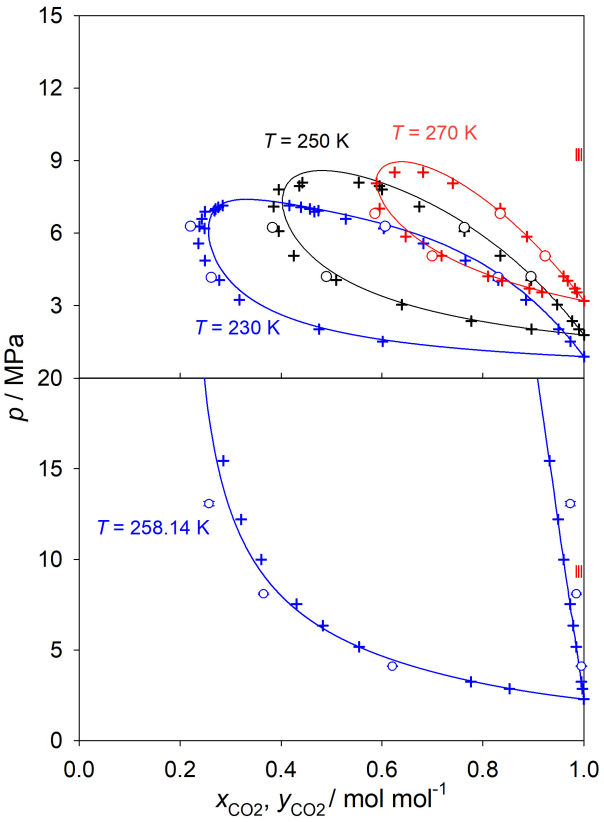

Figure S2: Vapor-liquid equilibria of CO_2 mixtures with hydrogen (bottom) or methane (top). Solid lines denote data from the GERG-2008 EOS[6] and crosses represent experimental data for CO_2 + hydrogen[11] and CO_2 + methane[12]. Circles depict molecular simulation results. Red vertical marks on the very right stand for the supercritical states of interest.

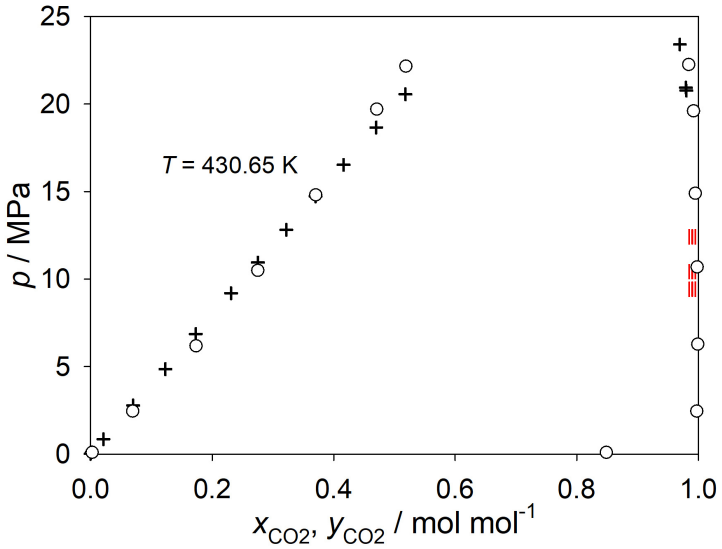

Figure S3: Vapor-liquid equilibria of CO_2 + naphthalene. Crosses represent experimental data[13], whereas circles depict molecular simulation results. Red vertical marks on the very right stand for the supercritical states of interest.

Finite size corrections

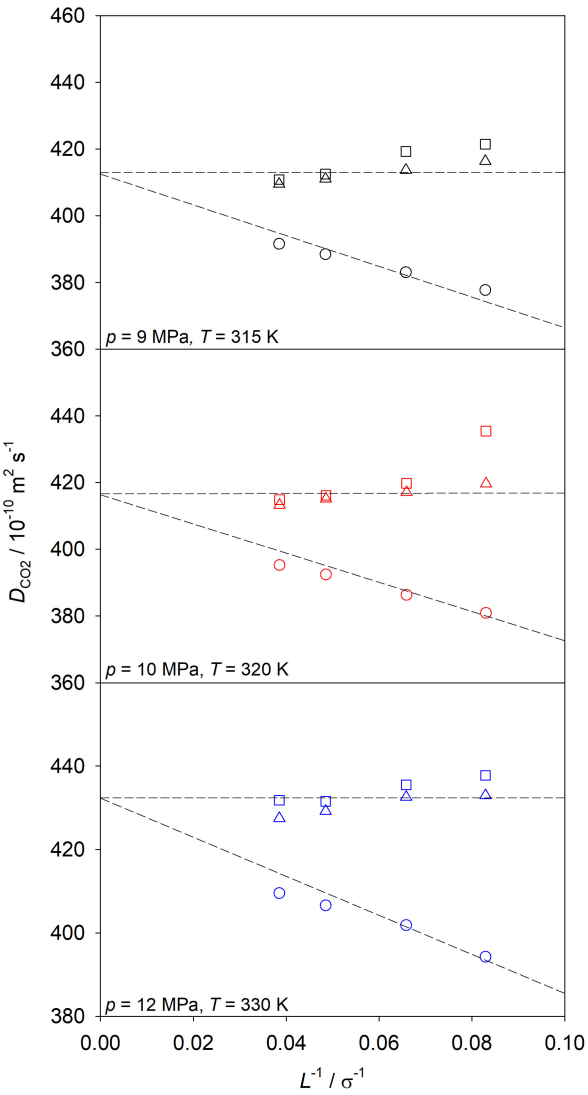

Figure S4: Finite size corrections of the intra-diffusion coefficient of CO_2 and its mixture with 1 mol% of benzene for three temperature-pressure pairs. Circles represent the original simulation data. Squares represent the intra-diffusion coefficients corrected with the approach of Yeh and Hummer[14] and the triangles represent data corrected with the approach of Leverant et al.[15].

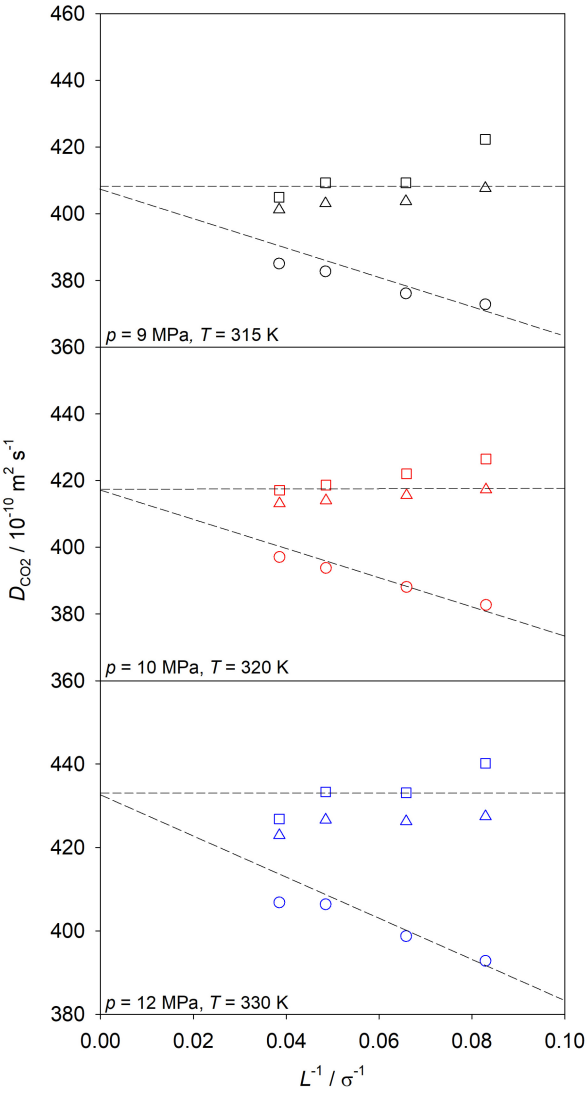

Figure S5: Finite size corrections of the intra-diffusion coefficient of CO_2 and its mixture with 1 mol% of toluene for three temperature-pressure pairs. Circles represent the original simulation data. Squares represent the intra-diffusion coefficients corrected with the approach of Yeh and Hummer[14] and the triangles represent data corrected with the approach of Leverant et al.[15].

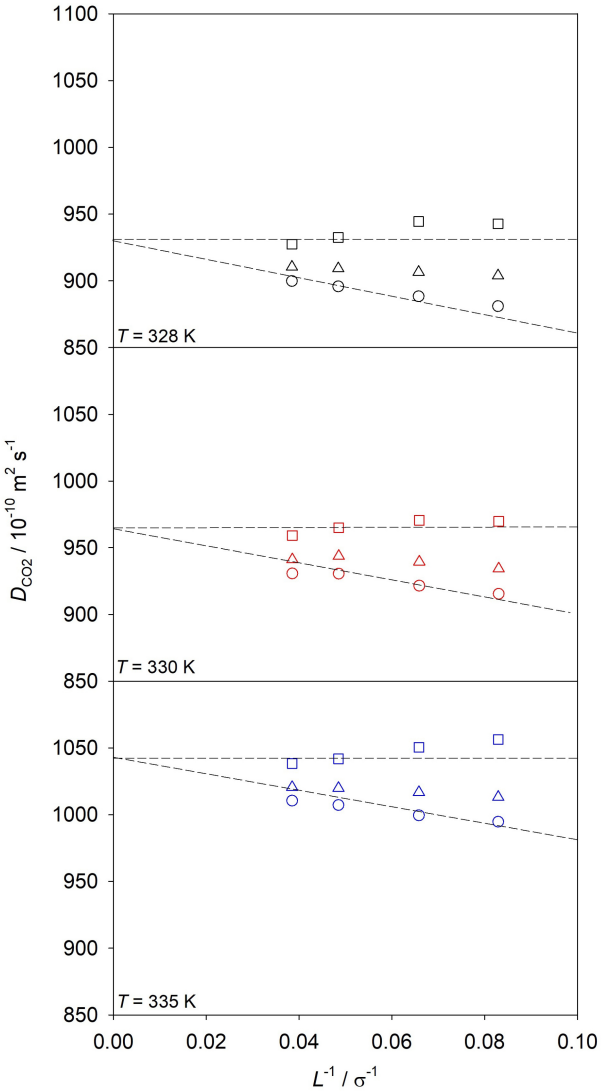

Figure S6: Finite size corrections of the intra-diffusion coefficient of CO_2 and its mixture with 1.5 (top), 1 (center) and 0.5 mol% (bottom) of ethane at three temperatures along $p = 9$ MPa. Circles represent the original simulation data. Squares represent the intra-diffusion coefficients corrected with the approach of Yeh and Hummer[14] and the triangles represent data corrected with the approach of Leverant et al.[15].

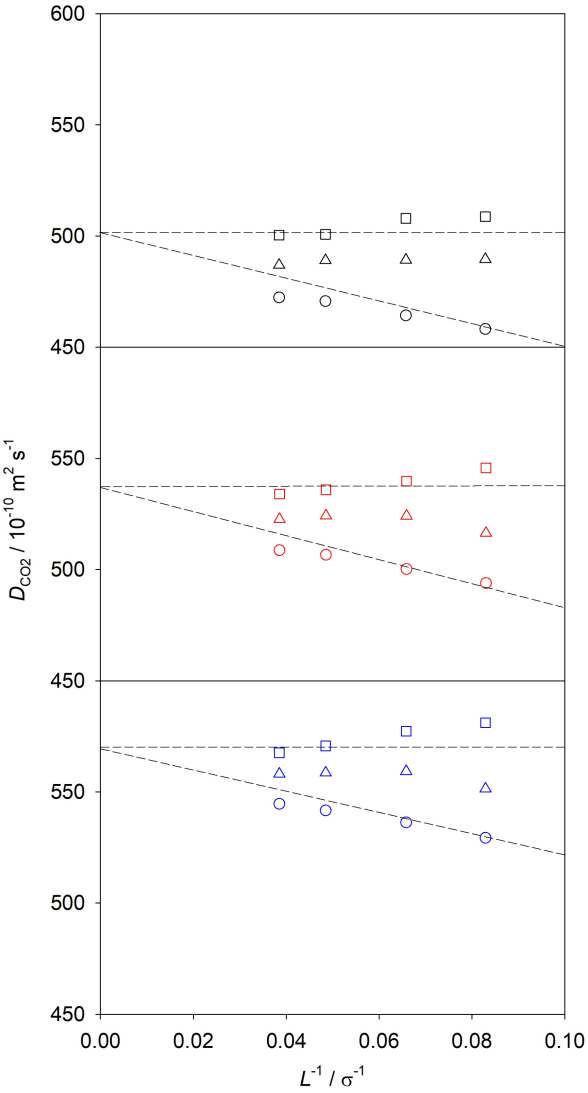

Figure S7: Finite size corrections of the intra-diffusion coefficient of CO_2 and its mixture with 1.5 (top), 1 (center) and 0.5 mol% (bottom) of isobutane along $p =$ 9 MPa and $T = 315$ K. Circles represent the original simulation data. Squares represent the intra-diffusion coefficients corrected with the approach of Yeh and Hummer[14] and the triangles represent data corrected with the approach of Leverant et al.[15].

Thermodynamic properties

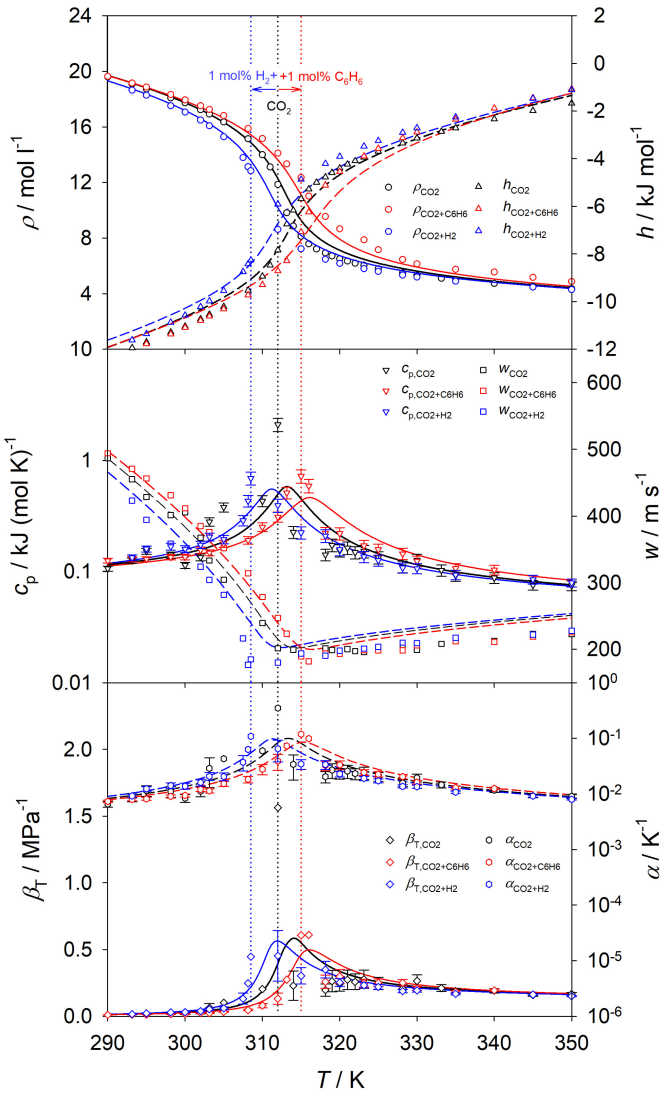

Figure S8: Temperature dependence of the thermodynamic properties of $scCO_2$ (black) and its mixtures with 1.0 mol% of hydrogen (blue) or benzene (red) at $p = 9$ MPa. Symbols show the present molecular simulation results. Density (circles) and enthalpy (triangles up) are shown at the top, isobaric heat capacity (triangles down) and speed of sound (squares) in the center, isothermal compressibility (diamonds) and volume expansivity (hexagons) at the bottom. Dashed and solid lines represent the EOS by Span and Wagner for CO_2 [16], the GERG-2008 EOS[6] for CO_2 + hydrogen and the mixture model by Blackham and Lemmon[17] for CO_2 + benzene. Dotted lines the Widom line temperature determined by the maximum of the isobaric heat capacity. Statistical uncertainties were omitted when they are either within symbol size or lead to visual clutter.

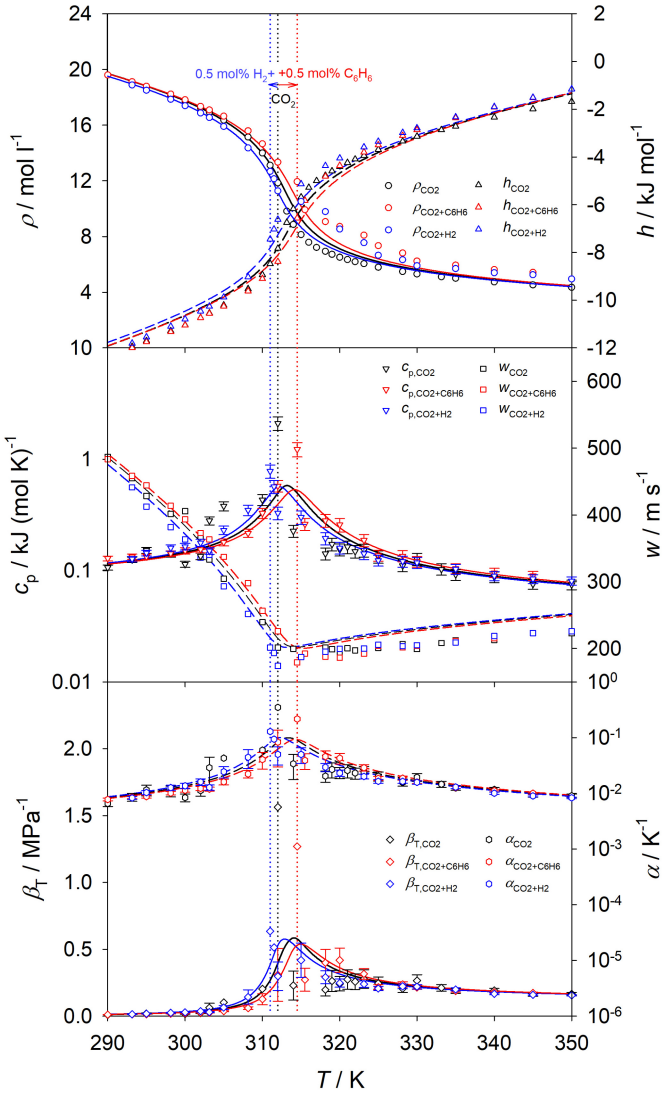

Figure S9: Temperature dependence of the thermodynamic properties of $scCO_2$ (black) and its mixtures with 0.5 mol% of hydrogen (blue) or benzene (red) at $p = 9$ MPa. Symbols show the present molecular simulation results. Density (circles) and enthalpy (triangles up) are shown at the top, isobaric heat capacity (triangles down) and speed of sound (squares) in the center, isothermal compressibility (diamonds) and volume expansivity (hexagons) at the bottom. Dashed and solid lines represent the EOS by Span and Wagner for CO_2 [16], the GERG-2008 EOS[6] for CO_2 + hydrogen and the mixture model by Blackham and Lemmon[17] for CO_2 + benzene. Dotted lines indicate the Widom line temperature determined by the maximum of the isobaric heat capacity. Statistical uncertainties were omitted when they are either within symbol size or lead to visual clutter.

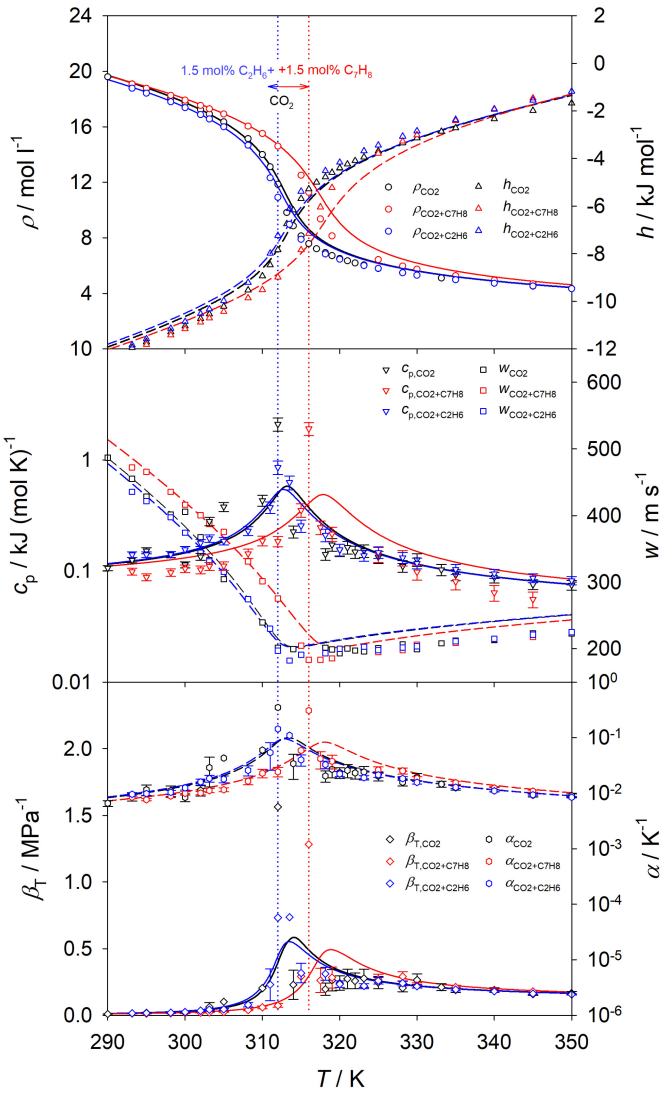

Figure S10: Temperature dependence of the thermodynamic properties of $scCO_2$ (black) and its mixtures with 1.5 mol% of ethane (blue) or toluene (red) at $p = 9$ MPa. Symbols show the present molecular simulation results. Density (circles) and enthalpy (triangles up) are shown at the top, isobaric heat capacity (triangles down) and speed of sound (squares) in the center, isothermal compressibility (diamonds) and volume expansivity (hexagons) at the bottom. Dashed and solid lines represent the EOS by Span and Wagner for CO_2 [16], the GERG-2008 EOS [6] for CO_2 + ethane and the mixture model by Blackham and Lemmon [17] for CO_2 + toluene. Dotted lines indicate the Widom line temperature determined by the maximum of the isobaric heat capacity. Statistical uncertainties were omitted when they are either within symbol size or lead to visual clutter.

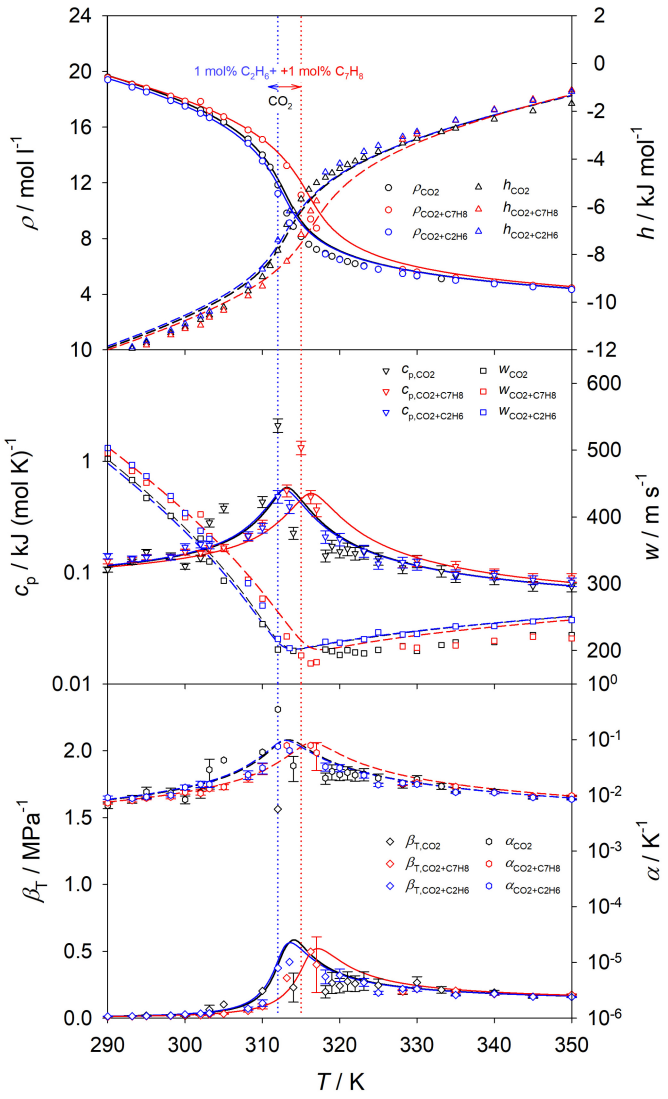

Figure S11: Temperature dependence of the thermodynamic properties of scCO$_2$ (black) and its mixtures with 1.0 mol% of ethane (blue) or toluene (red) at $p = 9$ MPa. Symbols show the present molecular simulation results. Density (circles) and enthalpy (triangles up) are shown at the top, isobaric heat capacity (triangles down) and speed of sound (squares) in the center, isothermal compressibility (diamonds) and volume expansivity (hexagons) at the bottom. Dashed and solid lines represent the EOS by Span and Wagner for CO$_2$ [16], the GERG-2008 EOS [6] for CO$_2$ + ethane and the mixture model by Blackham and Lemmon [17] for CO$_2$ + toluene. Dotted lines indicate the Widom line temperature determined by the maximum of the isobaric heat capacity. Statistical uncertainties were omitted when they are either within symbol size or lead to visual clutter.

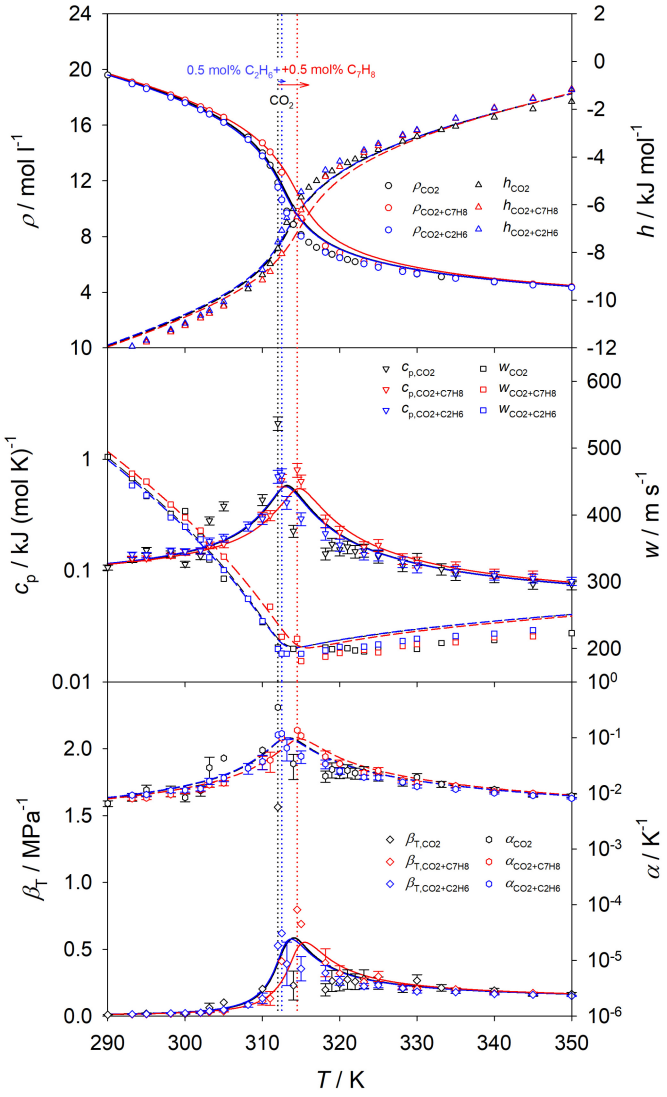

Figure S12: Temperature dependence of the thermodynamic properties of scCO$_2$ (black) and its mixtures with 0.5 mol% of ethane (blue) or toluene (red) at $p = 9$ MPa. Symbols show the present molecular simulation results. Density (circles) and enthalpy (triangles up) are shown at the top, isobaric heat capacity (triangles down) and speed of sound (squares) in the center, isothermal compressibility (diamonds) and volume expansivity (hexagons) at the bottom. Dashed and solid lines represent the EOS by Span and Wagner for CO$_2$ [16], the GERG-2008 EOS [6] for CO$_2$ + ethane and the mixture model by Blackham and Lemmon [17] for CO$_2$ + toluene. Dotted lines indicate the Widom line temperature determined by the maximum of the isobaric heat capacity. Statistical uncertainties were omitted when they are either within symbol size or lead to visual clutter.

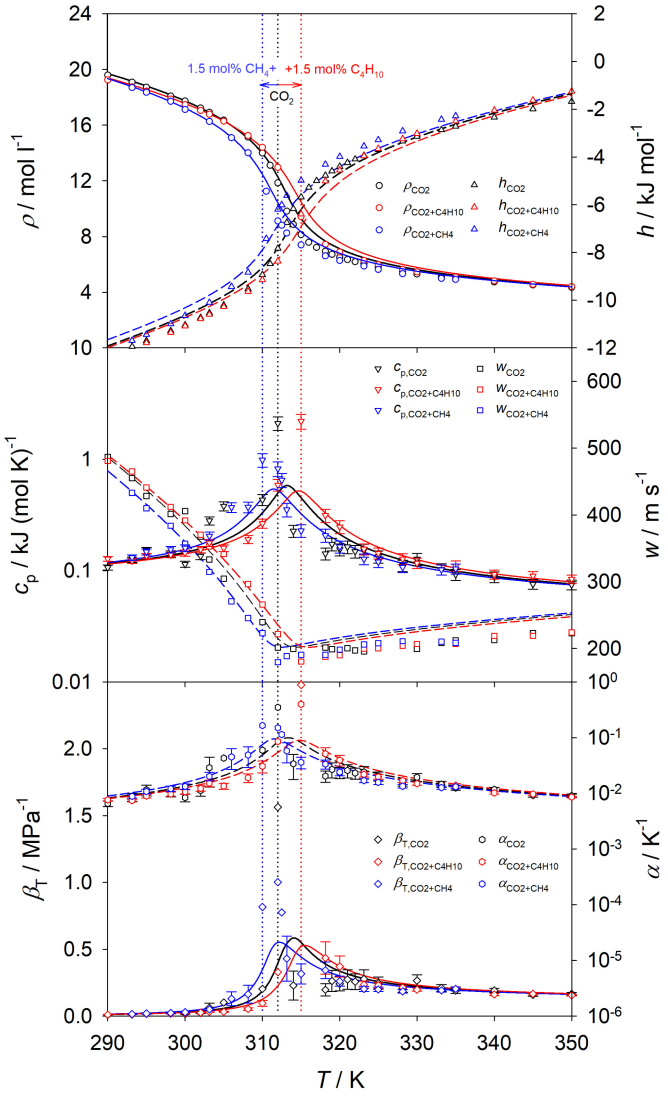

Figure S13: Temperature dependence of the thermodynamic properties of $scCO_2$ (black) and its mixtures with 1.5 mol% of methane (blue) or isobutane (red) at $p = 9$ MPa. Symbols show the present molecular simulation results. Density (circles) and enthalpy (triangles up) are shown at the top, isobaric heat capacity (triangles down) and speed of sound (squares) in the center, isothermal compressibility (diamonds) and volume expansivity (hexagons) at the bottom. Dashed and solid lines represent the EOS by Span and Wagner for CO_2 [16] and the GERG-2008 EOS[6] for CO_2 + methane or CO_2 + isobutane. Dotted lines indicate the Widom line temperature determined by the maximum of the isobaric heat capacity. Statistical uncertainties were omitted when they are either within symbol size or lead to visual clutter.

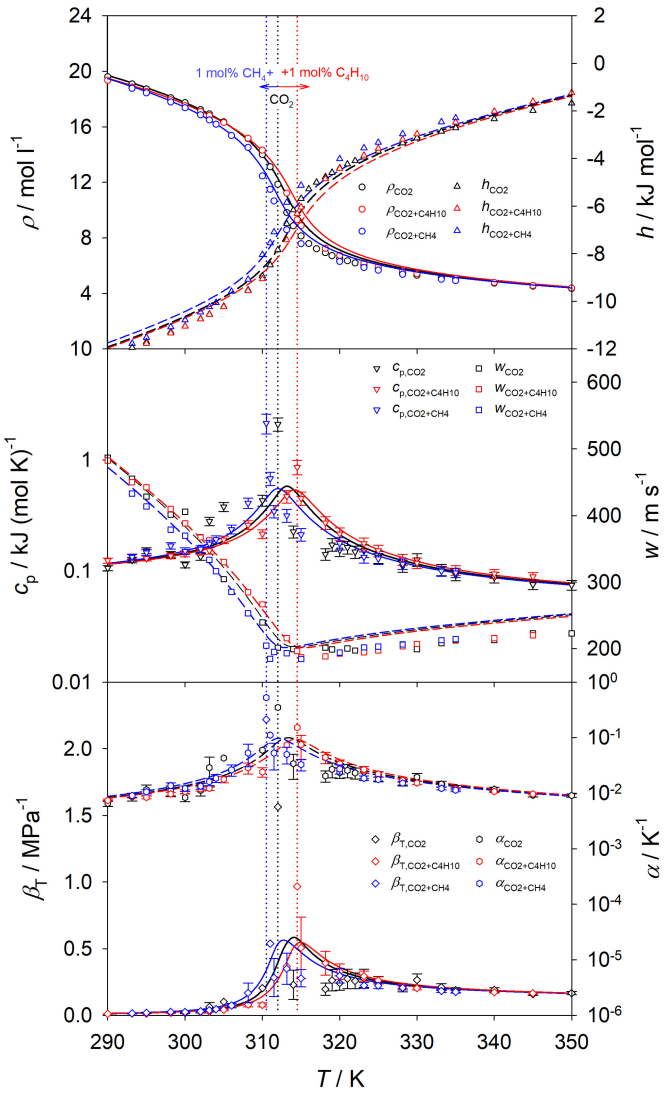

Figure S14: Temperature dependence of the thermodynamic properties of scCO$_2$ (black) and its mixtures with 1.0 mol% of methane (blue) or isobutane (red) at $p = 9$ MPa. Symbols show the present molecular simulation results. Density (circles) and enthalpy (triangles up) are shown at the top, isobaric heat capacity (triangles down) and speed of sound (squares) in the center, isothermal compressibility (diamonds) and volume expansivity (hexagons) at the bottom. Dashed and solid lines represent the EOS by Span and Wagner for CO$_2$ [16] and the GERG-2008 EOS [6] for CO$_2$ + methane or CO$_2$ + isobutane. Dotted lines indicate the Widom line temperature determined by the maximum of the isobaric heat capacity. Statistical uncertainties were omitted when they are either within symbol size or lead to visual clutter.

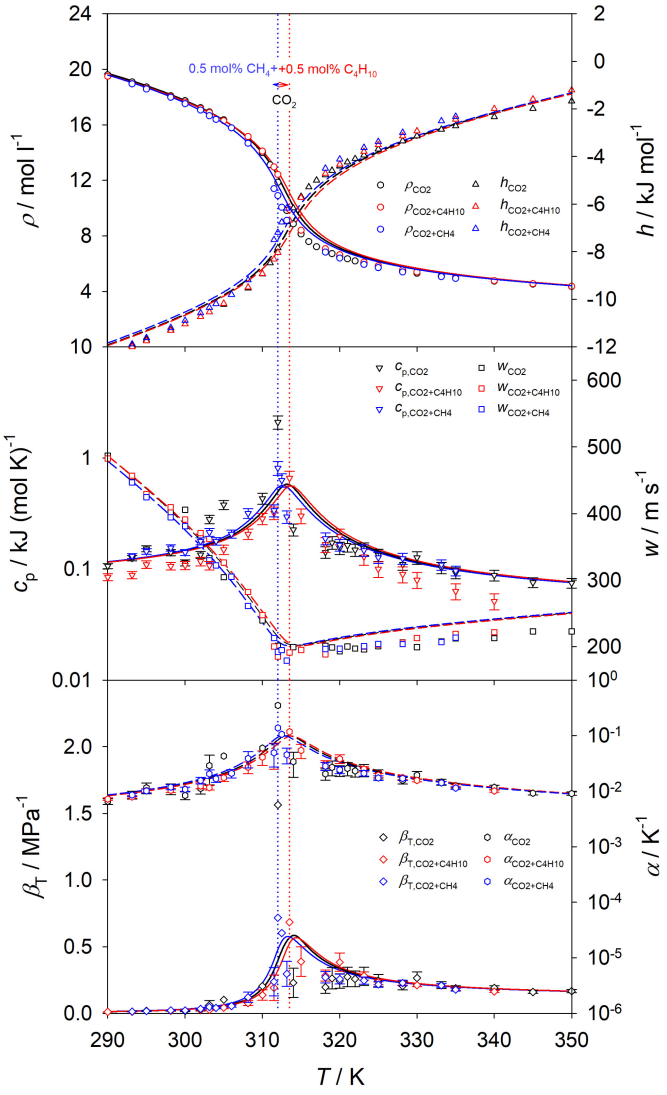

Figure S15: Temperature dependence of the thermodynamic properties of scCO$_2$ (black) and its mixtures with 0.5 mol% of methane (blue) or isobutane (red) at $p = 9$ MPa. Symbols show the present molecular simulation results. Density (circles) and enthalpy (triangles up) are shown at the top, isobaric heat capacity (triangles down) and speed of sound (squares) in the center, isothermal compressibility (diamonds) and volume expansivity (hexagons) at the bottom. Dashed and solid lines represent the EOS by Span and Wagner for CO$_2$ [16] and the GERG-2008 EOS [6] for CO$_2$ + methane or CO$_2$ + isobutane. Dotted lines indicate the Widom line temperature determined by the maximum of the isobaric heat capacity. Statistical uncertainties were omitted when they are either within symbol size or lead to visual clutter.

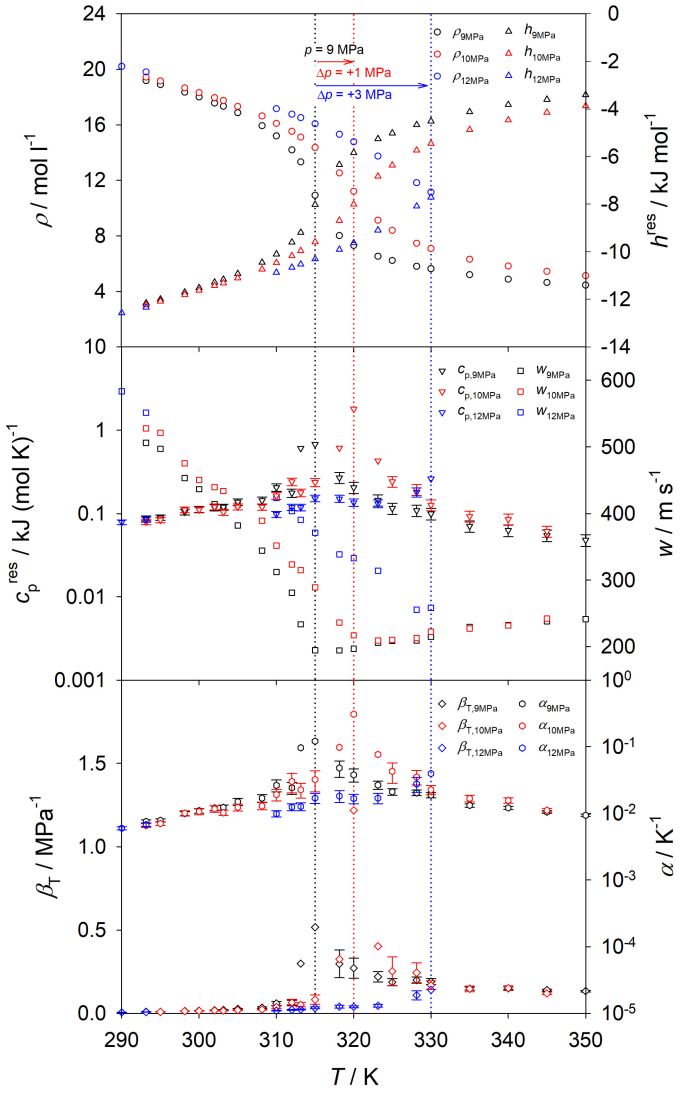

Figure S16: Temperature dependence of the thermodynamic properties of the $scCO_2$ mixture with 0.6 mol% of naphthalene at $p = 9$ MPa (black), 10 MPa (red) and 12 MPa (blue). Symbols show the present molecular simulation results. Density (circles) and residual enthalpy (triangles up) are shown at the top, residual isobaric heat capacity (triangles down) and speed of sound (squares) in the center, isothermal compressibility (diamonds) and volume expansivity (hexagons) at the bottom. Dotted lines indicate the Widom line temperature determined by the maximum of the isobaric heat capacity. Statistical uncertainties were omitted when they are either within symbol size or lead to visual clutter. No experimental or equation of state data were available for comparison.

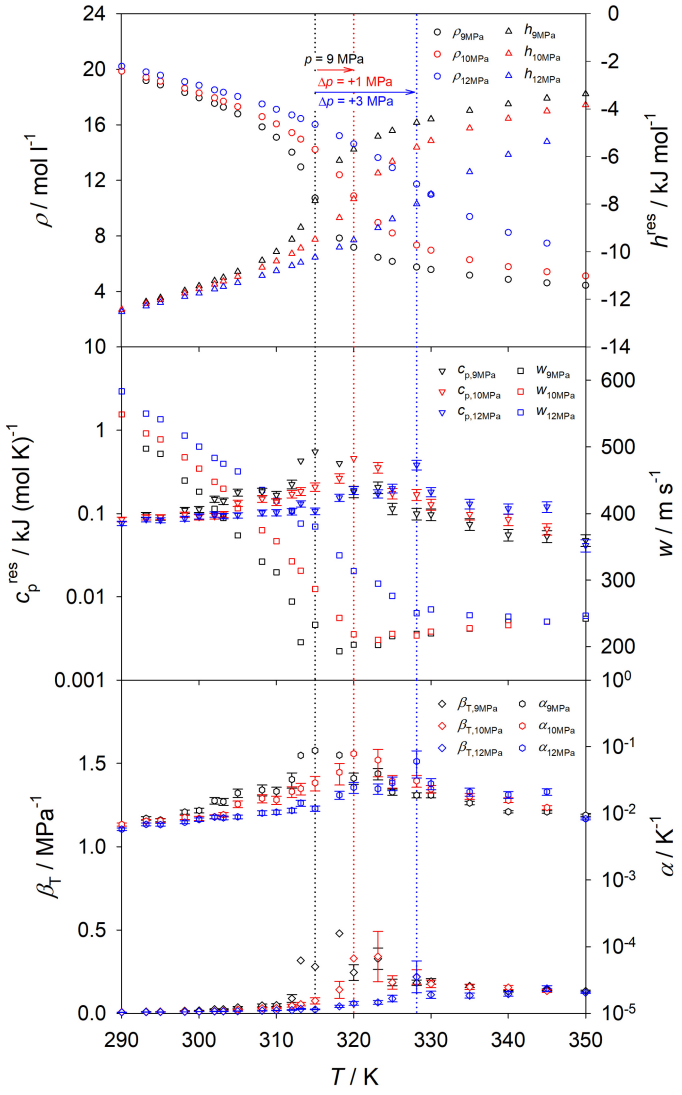

Figure S17: Temperature dependence of the thermodynamic properties of the $scCO_2$ mixture with 0.5 mol% of naphthalene at $p = 9$ MPa (black), 10 MPa (red) and 12 MPa (blue). Symbols show the present molecular simulation results. Density (circles) and residual enthalpy (triangles up) are shown at the top, residual isobaric heat capacity (triangles down) and speed of sound (squares) in the center, isothermal compressibility (diamonds) and volume expansivity (hexagons) at the bottom. Dotted lines indicate the Widom line temperature determined by the maximum of the isobaric heat capacity. Statistical uncertainties were omitted when they are either within symbol size or lead to visual clutter. No experimental or equation of state data were available for comparison.

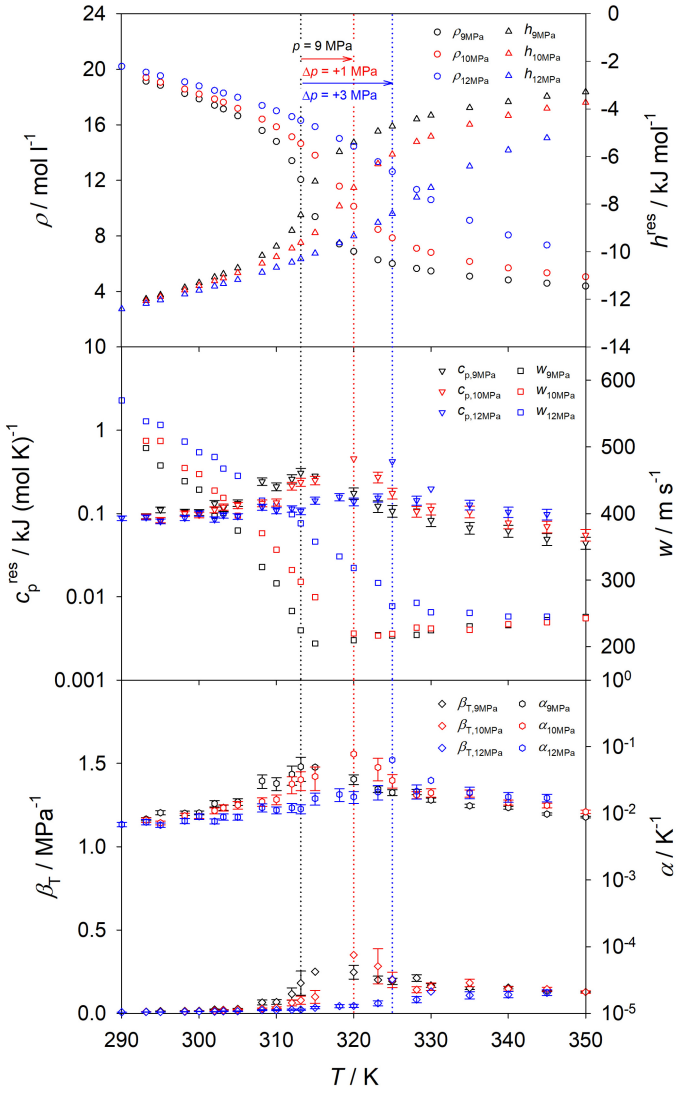

Figure S18: Temperature dependence of the thermodynamic properties of the $scCO_2$ mixture with 0.3 mol% of naphthalene at $p = 9$ MPa (black), 10 MPa (red) and 12 MPa (blue). Symbols show the present molecular simulation results. Density (circles) and residual enthalpy (triangles up) are shown at the top, residual isobaric heat capacity (triangles down) and speed of sound (squares) in the center, isothermal compressibility (diamonds) and volume expansivity (hexagons) at the bottom. Dotted lines indicate the Widom line temperature determined by the maximum of the isobaric heat capacity. Statistical uncertainties were omitted when they are either within symbol size or lead to visual clutter. No experimental or equation of state data were available for comparison.

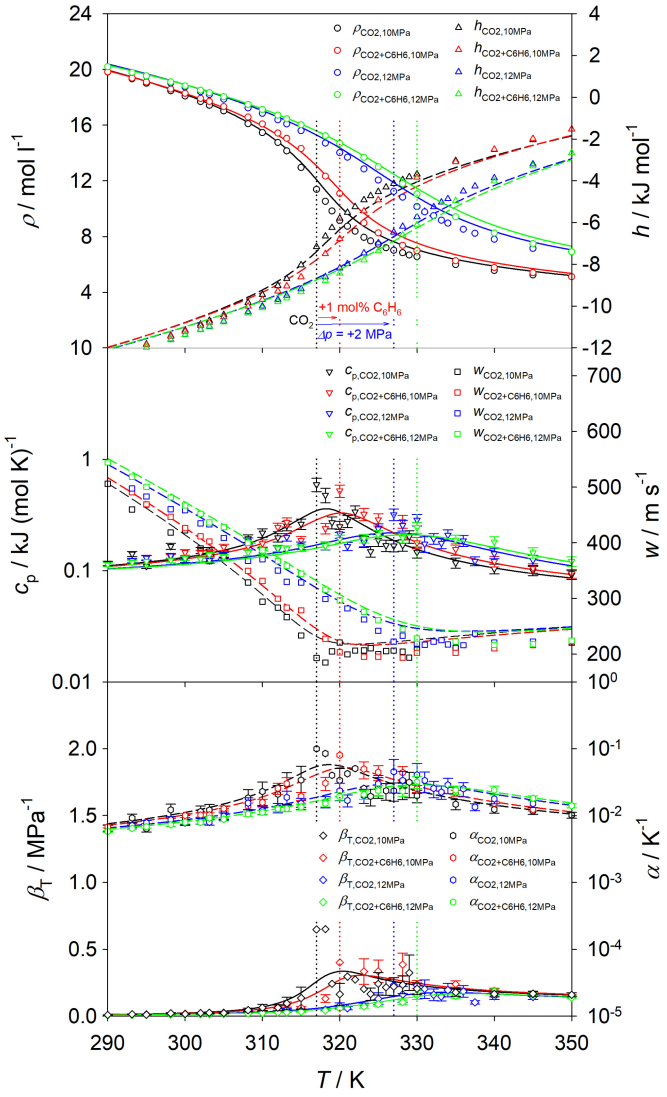

Figure S19: Temperature dependence of the thermodynamic properties of $scCO_2$ (black) and its mixture with 1.0 mol% benzene at $p = 10$ MPa (red) as well as $scCO_2$ (blue) and its mixture with 1.0 mol% benzene at $p = 12$ MPa (green). Symbols show the present molecular simulation results. Density (circles) and enthalpy (triangles up) are shown at the top, isobaric heat capacity (triangles down) and speed of sound (squares) in the center, isothermal compressibility (diamonds) and volume expansivity (hexagons) at the bottom. Dashed and solid lines represent the EOS by Span and Wagner EOS for CO_2[16] and the mixture model for by Blackham and Lemmon[17] for CO_2 + benzene. Dotted lines indicate the Widom line temperature determined by the maximum of the isobaric heat capacity. Statistical uncertainties were omitted when they are either within symbol size or lead to visual clutter.

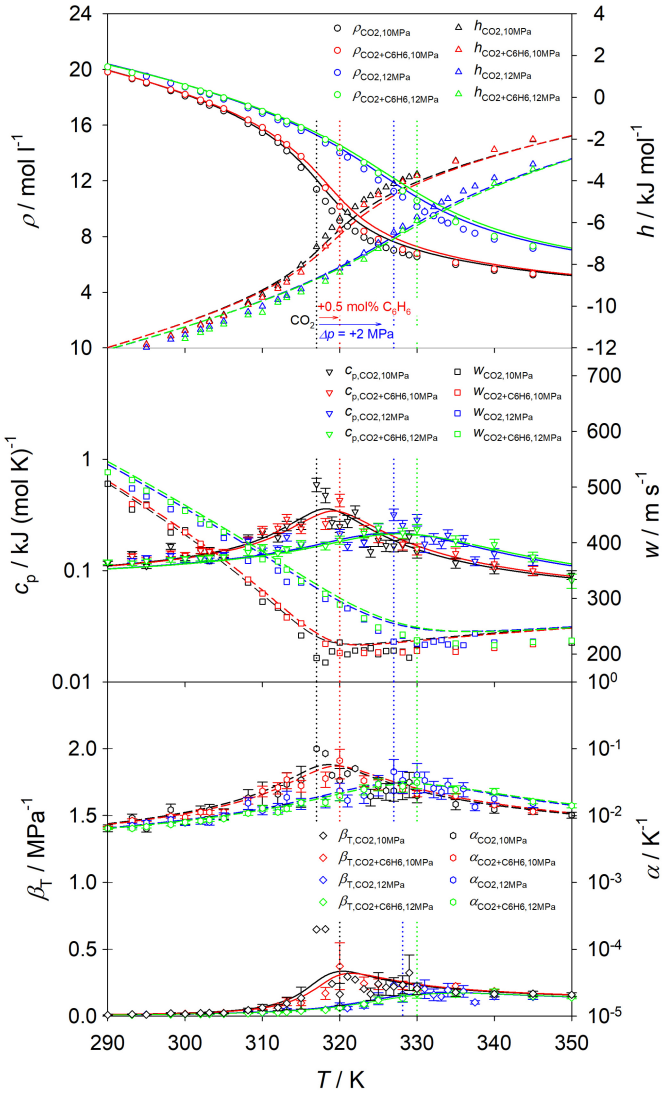

Figure S20: Temperature dependence of the thermodynamic properties of $scCO_2$ (black) and its mixture with 0.5 mol% benzene at $p = 10$ MPa (red) as well as $scCO_2$ (blue) and its mixture with 0.5 mol% benzene at $p = 12$ MPa (green). Symbols show the present molecular simulation results. Density (circles) and enthalpy (triangles up) are shown at the top, isobaric heat capacity (triangles down) and speed of sound (squares) in the center, isothermal compressibility (diamonds) and volume expansivity (hexagons) at the bottom. Dashed and solid lines represent the EOS by Span and Wagner EOS for CO_2[16] and the mixture model for by Blackham and Lemmon[17] for CO_2 + benzene. Dotted lines indicate the Widom line temperature determined by the maximum of the isobaric heat capacity. Statistical uncertainties were omitted when they are either within symbol size or lead to visual clutter.

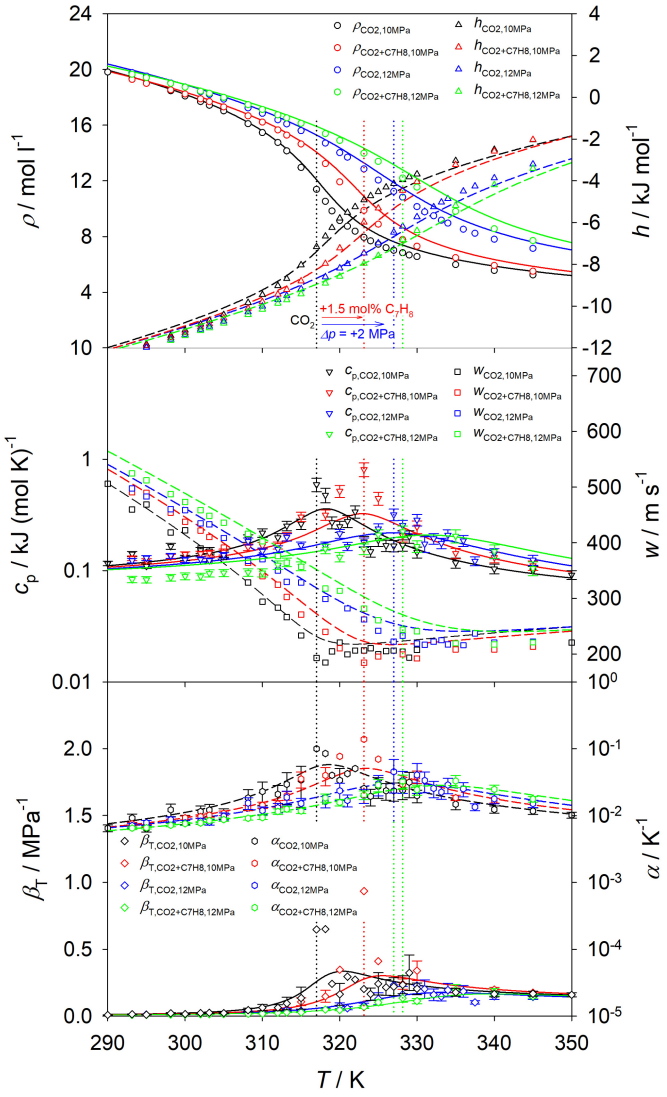

Figure S21: Temperature dependence of the thermodynamic properties of $scCO_2$ (black) and its mixture with 1.5 mol% toluene at $p = 10$ MPa (red) as well as $scCO_2$ (blue) and its mixture with 1.5 mol% toluene at $p = 12$ MPa (green). Symbols show the present molecular simulation results. Density (circles) and enthalpy (triangles up) are shown at the top, isobaric heat capacity (triangles down) and speed of sound (squares) in the center, isothermal compressibility (diamonds) and volume expansivity (hexagons) at the bottom. Dashed and solid lines represent the EOS by Span and Wagner EOS for CO_2[16] and the mixture model for by Blackham and Lemmon[17] for CO_2 + toluene. Dotted lines indicate the Widom line temperature determined by the maximum of the isobaric heat capacity. Statistical uncertainties were omitted when they are either within symbol size or lead to visual clutter.

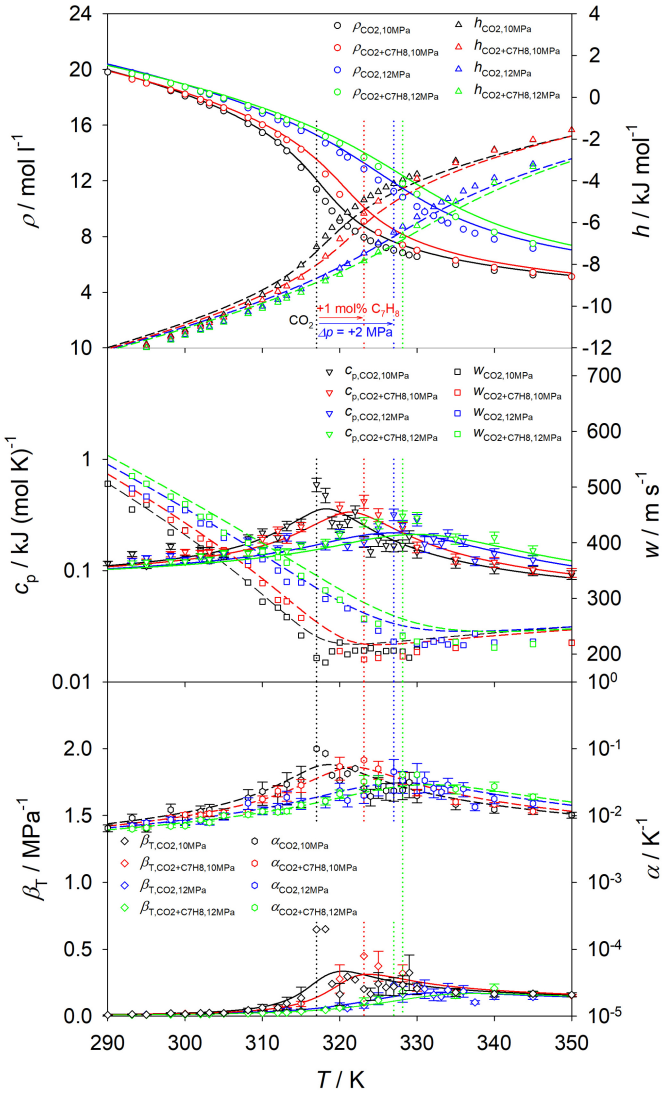

Figure S22: Temperature dependence of the thermodynamic properties of $scCO_2$ (black) and its mixture with 1.0 mol% toluene at $p = 10$ MPa (red) as well as $scCO_2$ (blue) and its mixture with 1.0 mol% toluene at $p = 12$ MPa (green). Symbols show the present molecular simulation results. Density (circles) and enthalpy (triangles up) are shown at the top, isobaric heat capacity (triangles down) and speed of sound (squares) in the center, isothermal compressibility (diamonds) and volume expansivity (hexagons) at the bottom. Dashed and solid lines represent the EOS by Span and Wagner EOS for CO_2[16] and the mixture model for by Blackham and Lemmon[17] for CO_2 + toluene. Dotted lines indicate the Widom line temperature determined by the maximum of the isobaric heat capacity. Statistical uncertainties were omitted when they are either within symbol size or lead to visual clutter.

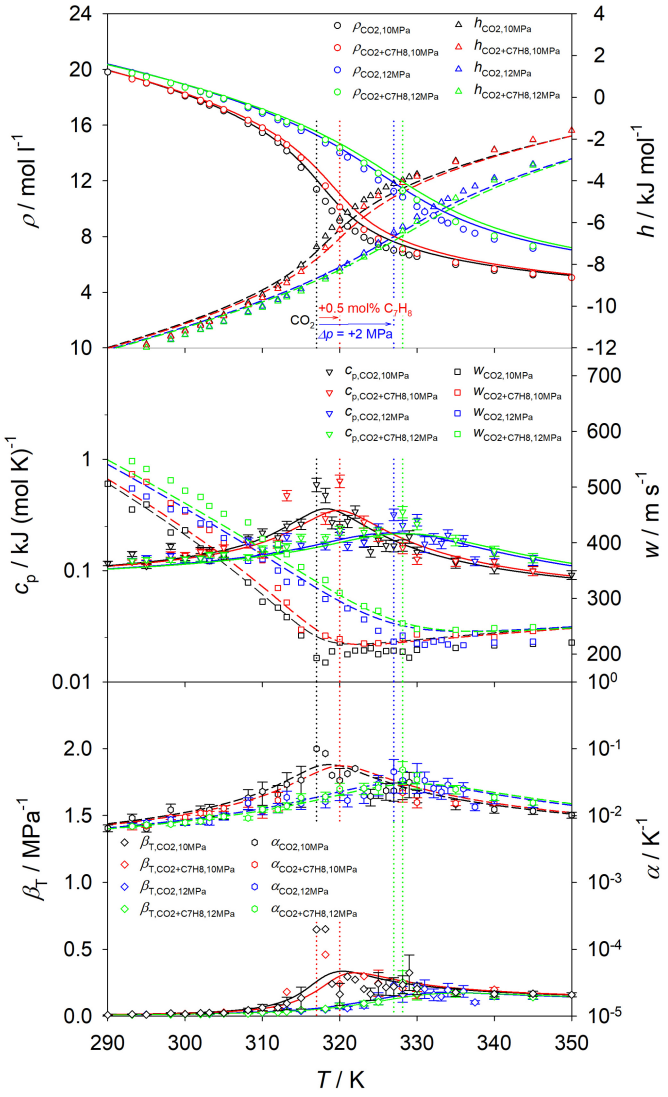

Figure S23: Temperature dependence of the thermodynamic properties of $scCO_2$ (black) and its mixture with 0.5 mol% toluene at $p = 10$ MPa (red) as well as $scCO_2$ (blue) and its mixture with 0.5 mol% toluene at $p = 12$ MPa (green). Symbols show the present molecular simulation results. Density (circles) and enthalpy (triangles up) are shown at the top, isobaric heat capacity (triangles down) and speed of sound (squares) in the center, isothermal compressibility (diamonds) and volume expansivity (hexagons) at the bottom. Dashed and solid lines represent the EOS by Span and Wagner EOS for CO_2[16] and the mixture model for by Blackham and Lemmon[17] for CO_2 + toluene. Dotted lines indicate the Widom line temperature determined by the maximum of the isobaric heat capacity. Statistical uncertainties were omitted when they are either within symbol size or lead to visual clutter.

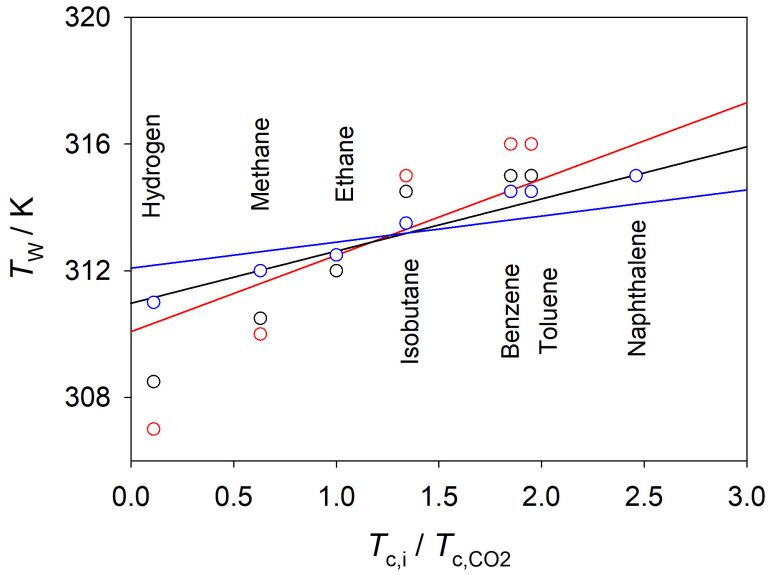

Figure S24: Widom line temperature of sCO_2 mixtures with 0.5 (blue), 1.0 (black) and 1.5 mol% (red) of the solute along the isobar $p = 9$ MPa over the ratio of the critical temperature of the solute to the critical temperature of pure CO_2. The Widom line temperature was determined by the isobaric heat capacity maximum. Circles represent calculations based on simulation data, solid lines show EOS data.

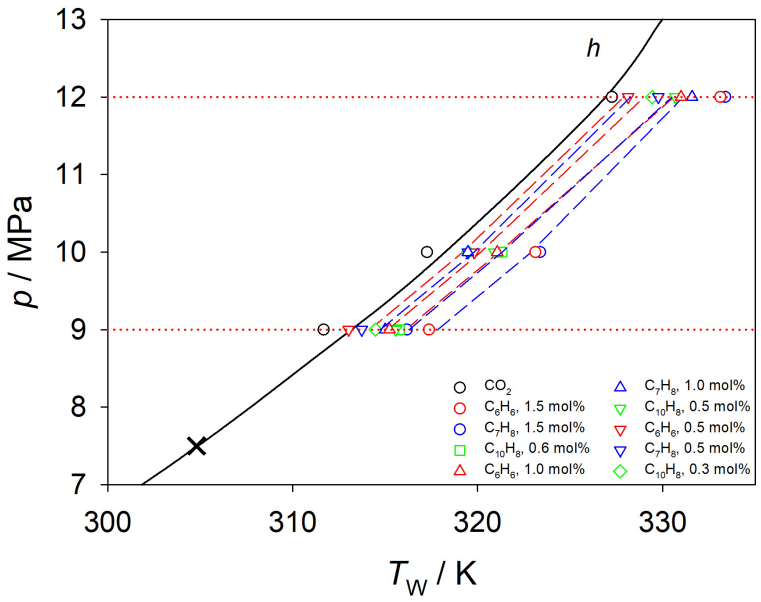

Figure S25: Pressure dependence of the Widom line temperature of $scCO_2$ (black) and its mixtures with 0.5, 1.0 and 1.5 mol% of benzene (red) or toluene (blue) as well as 0.3, 0.5 and 0.6 mol% of naphthalene (green). The Widom line temperature was determined by the inflection point of the enthalpy. Symbols represent simulation data. The solid line shows the Widom line determined from the EOS by Span and Wagner for CO_2 [16], dashed lines show the Widom line temperature of $scCO_2$ mixture with benzene (red) and toluene (black) calculated with the mixture models by Blackham and Lemmon [17]. Dotted lines (red) enclose the pressure range of interest. The critical point of CO_2 is represented by a cross.

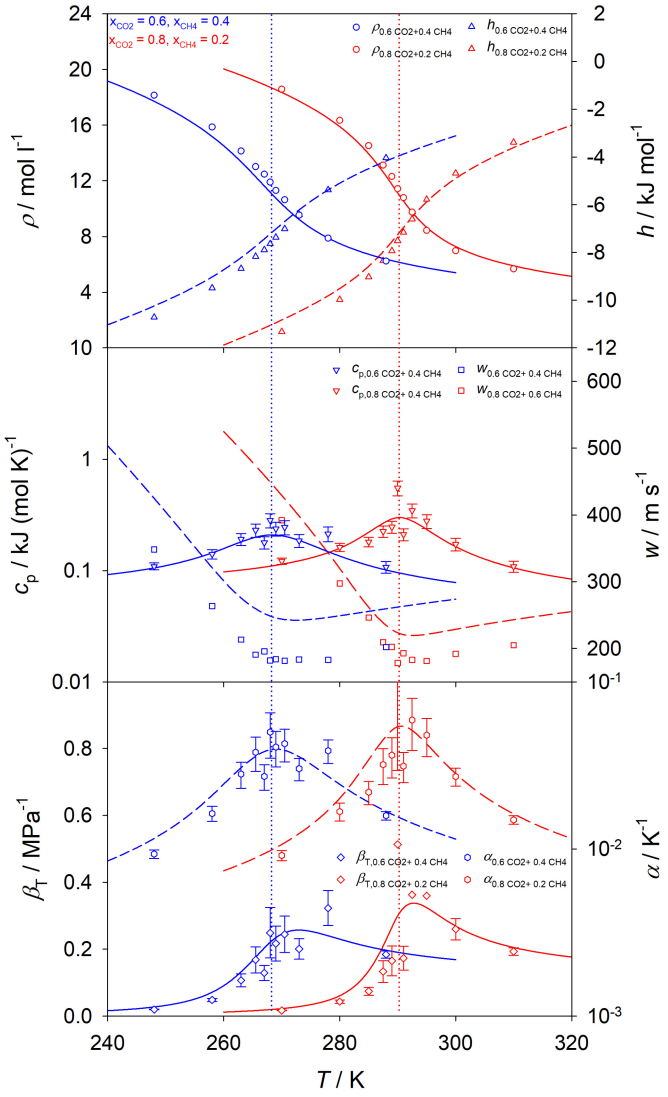

Figure S26: Temperature dependence of the thermodynamic properties of scCO$_2$ and its mixture with 20 mol% (red) and 40 mol% (blue) of methane at $p = 9$ MPa. Symbols show the present molecular simulation results. Density (circles) and enthalpy (triangles up) are shown at the top, isobaric heat capacity (triangles down) and speed of sound (squares) in the center, isothermal compressibility (diamonds) and volume expansivity (hexagons) at the bottom. Dashed and solid lines represent the GERG-2008 EOS[6] for CO$_2$ + methane. Dotted lines indicate the Widom line temperature determined by the maximum of the isobaric heat capacity from EOS. Statistical uncertainties were omitted when they are either within symbol size or lead to visual clutter.

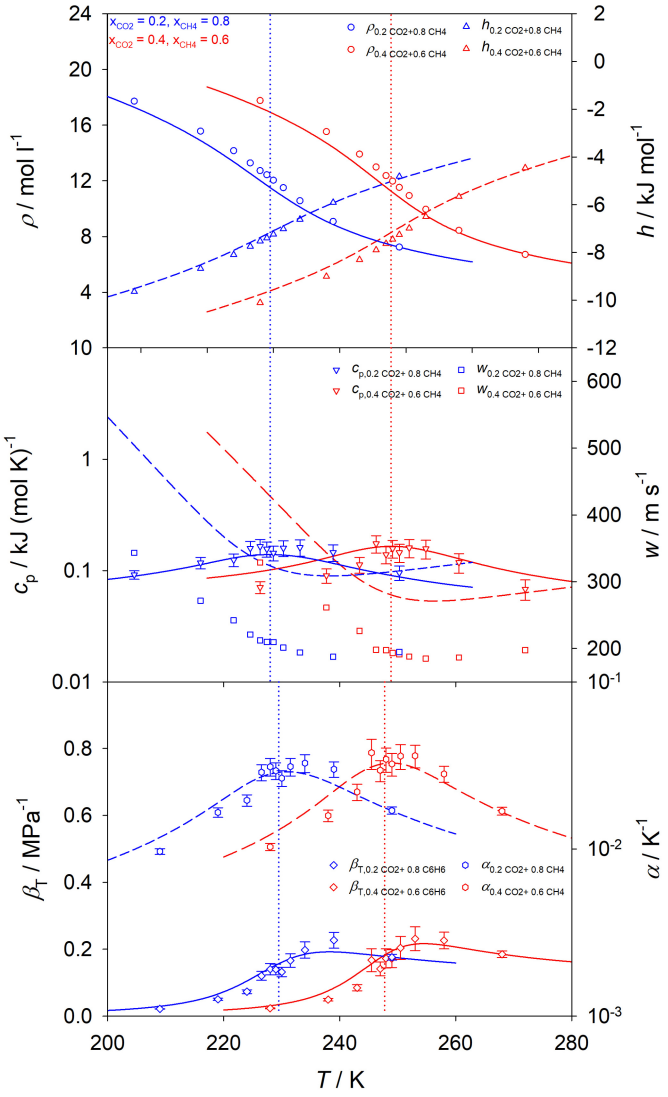

Figure S27: Temperature dependence of the thermodynamic properties of scCO$_2$ and its mixture with 60 mol% (red) and 80 mol% (blue) of methane at $p = 9$ MPa. Symbols show the present molecular simulation results. Density (circles) and enthalpy (triangles up) are shown at the top, isobaric heat capacity (triangles down) and speed of sound (squares) in the center, isothermal compressibility (diamonds) and volume expansivity (hexagons) at the bottom. Dashed and solid lines represent the GERG-2008 EOS[6] for CO$_2$ + methane. Dotted lines indicate the Widom line temperature determined by the maximum of the isobaric heat capacity from EOS. Statistical uncertainties were omitted when they are either within symbol size or lead to visual clutter.

Pseudo-boiling

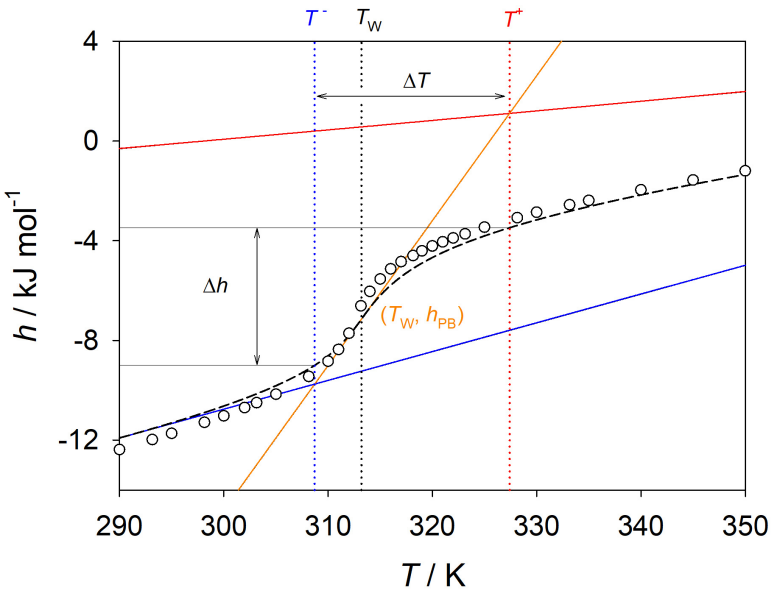

Figure S28: Analysis of pseudo-boiling with the approach of Banuti[18] for pure $scCO_2$. The underlying data for this analysis were taken from the EOS by Span and Wagner for CO_2[16]. Symbols depict molecular simulation data. Solid lines represent the asymptotes of the liquid enthalpy h^{L} (blue) and the ideal gas enthalpy h^{IG} (red). Dotted lines represent the pseudo-boiling start temperature T^{-} (blue), the Widom line temperature T_{W} (black) and the pseudo-boiling end temperature T^{+} (red). The Widom line temperature was determined by the maximum of the isobaric heat capacity. The pseudo-boiling start T^{-} (blue) and end T^{+} (red) temperatures were determined by the intersection point of the asymptote of the pseudo-boiling enthalpy h^{PB} (orange) with h^{L} and h^{IG}, respectively.

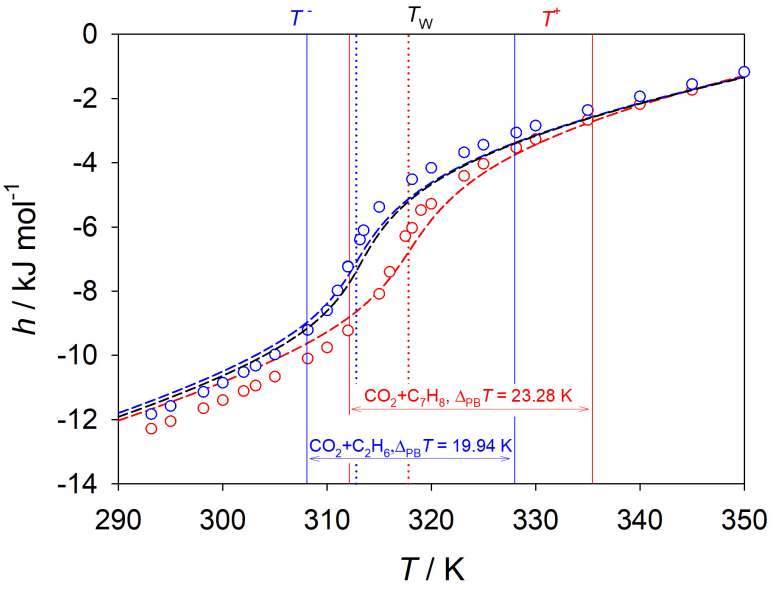

Figure S29: Pseudo-boiling of scCO$_2$ (black) and its mixtures with 1.5 mol% of ethane (blue) or toluene (red) along the isobar $p = 9$ MPa. Circles represent simulation data. Dashed lines represent the EOS by Span and Wagner for CO$_2$[16], the GERG-2008 EOS[6] for CO$_2$ + ethane and the mixture model by Blackham and Lemmon[17] for CO$_2$ + toluene. The Widom line temperature is indicated by the dotted lines. The pseudo-boiling start T^- and end T^+ temperatures enclose the extended Widom region as depicted by solid lines.

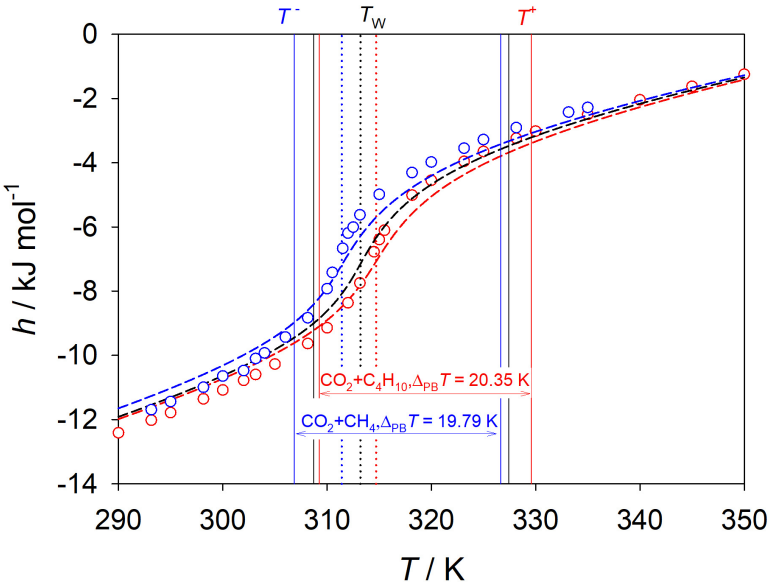

Figure S30: Pseudo-boiling of scCO$_2$ (black) and its mixtures with 1.5 mol% of methane (blue) or isobutane (red) along the isobar $p = 9$ MPa. Circles represent simulation data. Dashed lines represent the EOS by Span and Wagner for CO$_2$ [16] and the GERG-2008 EOS [6] for CO$_2$ + methane and CO$_2$ + isobutane. The Widom line temperature is indicated by the dotted lines. The pseudo-boiling start T^- and end T^+ temperatures enclose the extended Widom region as depicted by solid lines.

Table S2: Quantitative analysis of pseudo-boiling on basis of EOS data for the studied CO_2 mixtures with 0.5, 1.0 and 1.5 mol% of the solute along the isobar $p = 9$ MPa. The scCO_2 mixtures with benzene and toluene were additionally analyzed at $p = 10$ MPa and 12 MPa. The Widom line temperature was determined by the isobaric heat capacity maximum.

9 MPa 1.5mol%	T_W / K	T^- / K	T^+/ K	$\Delta_{PB}T$ / K	$\Delta_{PB}h$ / kJ mol^{-1}	$\frac{\Delta_{st}h}{\Delta_{th}h}$
CO_2	313.20	308.72	327.41	18.70	5.52	2.56
hydrogen	310.20	305.73	325.37	19.64	5.48	2.32
methane	311.40	306.85	326.64	19.79	5.56	2.37
ethane	312.80	308.07	328.01	19.94	5.61	2.42
isobutane	314.60	309.25	329.59	20.35	5.70	2.44
benzene	316.20	310.26	334.95	24.68	6.24	2.25
toluene	317.80	312.14	335.42	23.28	6.09	2.36
9 MPa 1 mol%	T_W / K	T^- / K	T^+ / K	$\Delta_{PB}T$ / K	$\Delta_{PB}h$ / kJ mol^{-1}	$\frac{\Delta_{st}h}{\Delta_{th}h}$
hydrogen	311.20	306.73	326.06	19.34	5.50	2.40
methane	312.00	307.49	326.98	19.49	5.56	2.43
ethane	312.90	308.23	327.76	19.53	5.58	2.46
isobutane	314.20	308.97	328.49	19.52	5.63	2.51
benzene	315.20	309.81	332.49	22.68	5.98	2.33
toluene	316.20	310.96	332.71	21.75	5.92	2.42
9 MPa 0.5 mol%	T_W / K	T^- / K	T^+ / K	$\Delta_{PB}T$ / K	$\Delta_{PB}h$ / kJ mol^{-1}	$\frac{\Delta_{st}h}{\Delta_{th}h}$
hydrogen	312.20	307.71	326.73	19.02	5.51	2.48
methane	312.60	308.09	327.18	19.09	5.55	2.50
ethane	313.00	308.52	327.63	19.11	5.54	2.50
isobutane	313.60	308.52	327.63	19.11	5.61	2.55
benzene	314.20	309.20	327.63	20.70	5.77	2.44
toluene	314.80	309.89	330.11	20.22	5.73	2.49
10 MPa 1.5 mol%	T_W / K	T^- / K	T^+ / K	$\Delta_{PB}T$ / K	$\Delta_{PB}h$ / kJ mol^{-1}	$\frac{\Delta_{st}h}{\Delta_{th}h}$
CO_2	318.20	310.64	342.26	31.62	6.30	2.25
benzene	321.20	309.92	346.82	36.90	6.47	1.91
toluene	323.00	313.78	350.41	36.63	6.06	2.03
10 MPa 1 mol%	T_W / K	T^- / K	T^+ / K	$\Delta_{PB}T$ / K	$\Delta_{PB}h$ / kJ mol^{-1}	$\frac{\Delta_{st}h}{\Delta_{th}h}$
benzene	320.20	311.53	347.24	35.71	6.20	2.02
toluene	321.40	312.75	347.71	34.96	6.08	2.10
10 MPa 0.5 mol%	T_W / K	T^- / K	T^+ / K	$\Delta_{PB}T$ / K	$\Delta_{PB}h$ / kJ mol^{-1}	$\frac{\Delta_{st}h}{\Delta_{th}h}$
benzene	319.20	311.06	344.73	33.67	6.27	2.13
toluene	319.80	311.64	344.94	33.30	6.21	2.17
12 MPa 1.5 mol%	T_W / K	T^- / K	T^+ / K	$\Delta_{PB}T$ / K	$\Delta_{PB}h$ / kJ mol^{-1}	$\frac{\Delta_{st}h}{\Delta_{th}h}$
CO_2	326.90	313.33	370.00	56.67	8.32	1.11
benzene	329.60	314.65	377.72	63.07	8.77	1.01
toluene	331.60	316.29	378.55	62.26	8.73	1.05
12 MPa 1 mol%	T_W / K	T^- / K	T^+ / K	$\Delta_{PB}T$ / K	$\Delta_{PB}h$ / kJ mol^{-1}	$\frac{\Delta_{st}h}{\Delta_{th}h}$
benzene	328.80	314.24	375.07	60.83	8.55	1.04
toluene	330.00	315.24	375.69	60.45	8.54	1.07
12 MPa 0.5 mol%	T_W / K	T^- / K	T^+ / K	$\Delta_{PB}T$ / K	$\Delta_{PB}h$ / kJ mol^{-1}	$\frac{\Delta_{st}h}{\Delta_{th}h}$
benzene	327.80	313.77	372.52	58.75	8.36	1.07
toluene	328.40	314.20	372.78	58.58	8.35	1.09

Table S3: Widom line temperature of the studied $scCO_2$ mixtures determined by six criteria along the isobar $p = 9$ MPa. The mixture $scCO_2$ + naphthalene was studied at solute mole fractions 0.3, 0.5 and 0.6 mol%.

solute mole fraction	maximum of c_p (EOS)			maximum of c_p (SIM)		
criterion	0.005	0.01	0.015	0.005	0.01	0.015
CO_2	313.2			312.0		
hydrogen	312.2	311.2	310.2	311	308.5	307
methane	312.6	312	311.4	312	310	310.5
ethane	313	312.9	312.8	312.5	312	312
isobutane	313.6	314.2	314.6	313.5	314.5	315
benzene	314.2	315.2	316.1	314.5	315	316
toluene	314.8	316.2	317.8	314.5	315	316
naphthalene	-			315	315	313.2
criterion	$\eta_{cc} = \eta_{kk}$			minimum of ν		
CO_2	313.15			314.00		
hydrogen	311.5	310	309.5	311	310	308.1
methane	312.5	312	311.5	312.5	312	310
ethane	312.5	312	311.5	313.5	312	311
isobutane	313.5	314	314.5	313.2	315	315.5
benzene	314.5	315.5	317	315.5	316	317.5
toluene	314.5	316	317	315	314.5	316.2
naphthalene	314.5	315.5	316	315.0	315.5	313.2
criterion	inflection of h (SIM)			inflection of D_i		
CO_2	-			315.10		
hydrogen	310.6	308.8	307.2	314.4	313.8	312.2
methane	312	310.8	310.5	313.5	313	312.3
ethane	312.2	311.9	311.8	315.5	315.3	312.7
isobutane	313.2	313.9	314.4	316.1	316.7	317.1
benzene	314.5	315.6	317	316.8	319.2	320.2
toluene	314.4	316.2	316.5	317.9	319.6	320.9
naphthalene	314.5	315.6	315.8	322.9	320	326.2

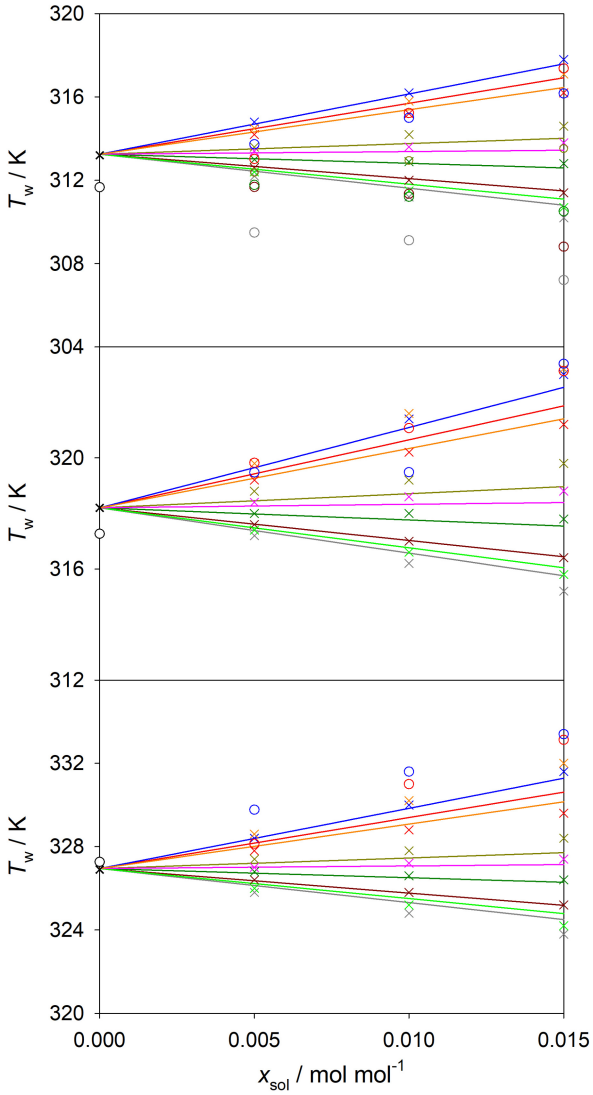

Figure S31: Widom line temperature of $scCO_2$ and its mixture with hydrogen (grey), nitrogen (green), methane (dark red), ethane (dark green), propane (pink), isobutane (dark yellow), heptane (orange), benzene (red) or toluene (blue) along the isobars $p = 9$ MPa (top), 10 MPa (center) and 12 MPa (bottom). Solid lines represent the results of the equation proposed in this work: $T_{\mathrm{w}}(p, x_{\mathrm{sol}}) = T_{\mathrm{c,CO2}}\,(p/p_{\mathrm{c,CO2}})^{0.1487} + x_{\mathrm{sol}}\,[119.8\cdot(T_{\mathrm{c,i}}/T_{\mathrm{c,CO2}})^2 - 164.6]$. Crosses represent the mixture model by Blackham and Lemmon[17] for CO_2 mixtures with benzene or toluene, and the GERG-2008 EOS[6] for the remaining mixtures. Circles depict simulation data.

Transport properties

Intra-diffusion coefficients

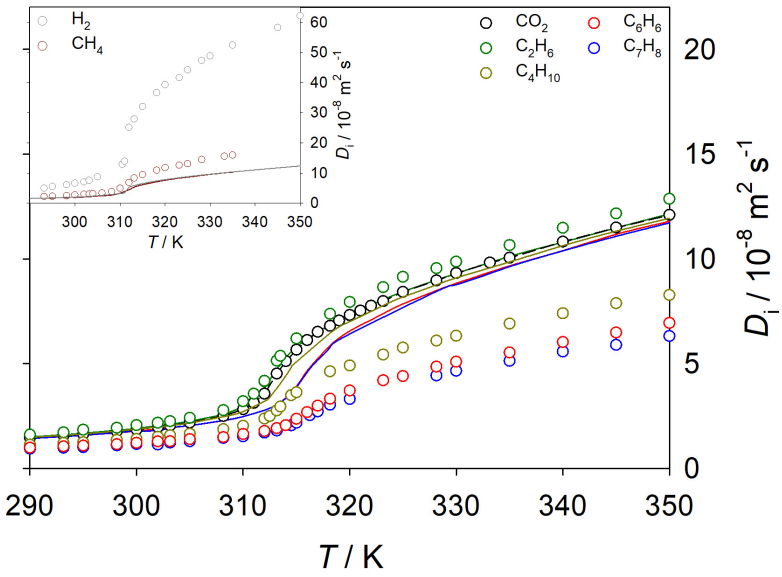

Figure S32: Temperature dependence of the intra-diffusion coefficients of binary mixtures of $scCO_2$ (black) with 1 mol% of ethane (dark green), isobutane (dark yellow), benzene (red), toluene (blue) or naphthalene (green) along the isobar $p = 9$ MPa. Circles represent the intra-diffusion coefficient of the solute and solid lines represent the intra-diffusion coefficient of $scCO_2$. The inset shows the results for hydrogen (grey) and methane (dark red) over a larger intra-diffusion coefficient range.

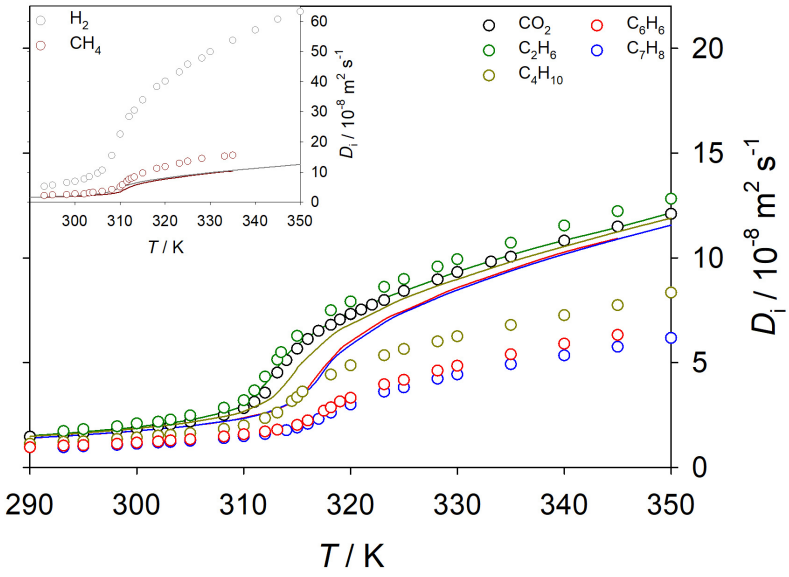

Figure S33: Temperature dependence of the intra-diffusion coefficients of binary mixtures of $scCO_2$ (black) with 1.5 mol% of ethane (dark green), isobutane (dark yellow), benzene (red), toluene (blue) or naphthalene (green) along the isobar $p = 9$ MPa. Circles represent the intra-diffusion coefficient of the solute and solid lines represent the intra-diffusion coefficient of $scCO_2$. The inset shows the results for hydrogen (grey) and methane (dark red) over a larger intra-diffusion coefficient range.

Shear viscosity

The kinetic η_{kk}, configurational η_{cc} and kinetic-configurational η_{kc} contributions to the shear viscosity are given by:

$$\eta_{\mathrm{kk}} = \frac{1}{Vk_BT}\int_0^\infty dt\, \Big\langle \sum_{i=1}^{N} m_i v_i^x(t) v_i^y(t) \cdot \sum_{i=1}^{N} m_i v_i^x(0) v_i^y(0) \Big\rangle, \tag{S2}$$

$$\eta_{\mathrm{cc}} = \frac{1}{4Vk_BT}\int_0^\infty dt\, \left\langle \sum_{i=1}^{N}\sum_{j\neq i}^{N} r_{ij}^x(t)\frac{\partial u_{ij}(t)}{\partial r_{ij}^y} \cdot \sum_{i=1}^{N}\sum_{j\neq i}^{N} r_{ij}^x(0)\frac{\partial u_{ij}(0)}{\partial r_{ij}^y} \right\rangle, \tag{S3}$$

$$\begin{aligned}\eta_{kc} = -\frac{1}{2Vk_BT}\int_0^\infty dt\, \Bigg\langle & \sum_{i=1}^{N} m_i v_i^x(0) v_i^y(0) \cdot \sum_{i=1}^{N}\sum_{j\neq i}^{N} r_{ij}^x(t)\frac{\partial u_{ij}(t)}{\partial r_{ij}^y} \\ & + \sum_{i=1}^{N} m_i v_i^x(t) v_i^y(t) \cdot \sum_{i=1}^{N}\sum_{j\neq i}^{N} r_{ij}^x(0)\frac{\partial u_{ij}(0)}{\partial r_{ij}^y} \Bigg\rangle,\end{aligned} \tag{S4}$$

where V stands for the volume, T for the temperature and i and j denote different molecules of any species that interact with the potential u. The upper indices x and y stand for the spatial vector components, e.g., for velocity v_i^x or site-site distance r_{ij}^x.

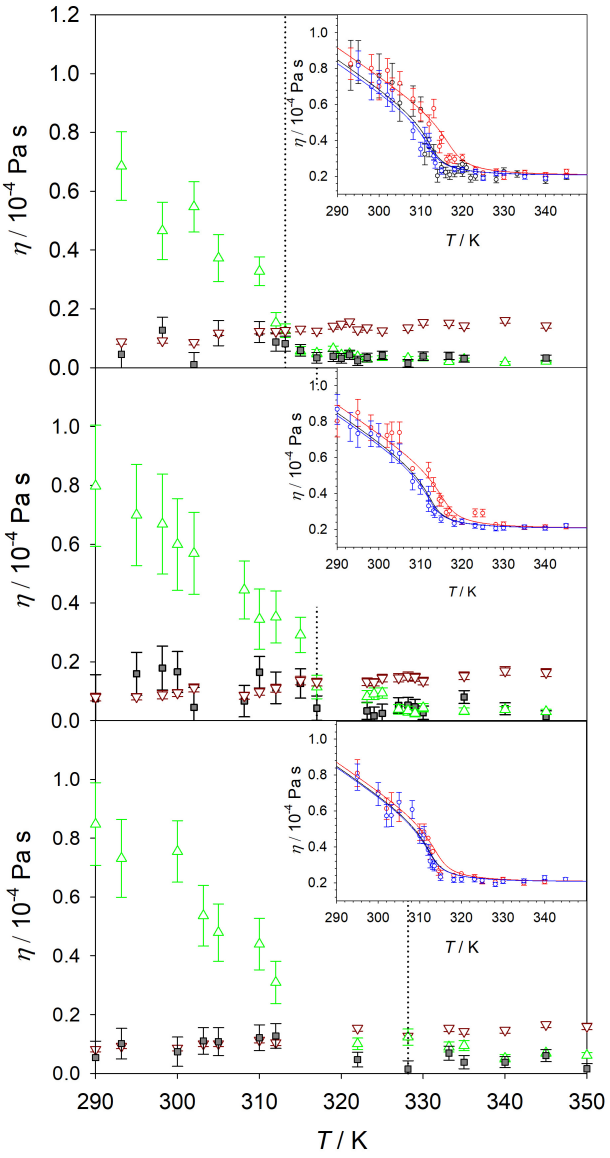

Figure S34: Temperature dependence of the kinetic η_{kk} (brown triangles), configurational η_{cc} (green triangles) and kinetic-configurational η_{kc} (grey squares) contributions to the shear viscosity of $scCO_2$ along the isobar $p = 9$ MPa (top), 10 MPa (center) and 12 MPa (bottom). The dotted line indicates the Widom line temperature calculated with the criterion of Bell et al.[19]. The inset shows the temperature dependence of the shear viscosity of $scCO_2$ (red) and its mixtures with 0.5 (top), 1 (center) and 1.5 mol % (bottom) of ethane (blue) or toluene (red) along the isobar $p = 9$ MPa. In the inset, circles show simulation data and solid lines EOS data. The reference correlation for the shear viscosity by Laesecke et al.[20] was used for pure $scCO_2$. An extended corresponding states approach[21] was used for the mixtures.

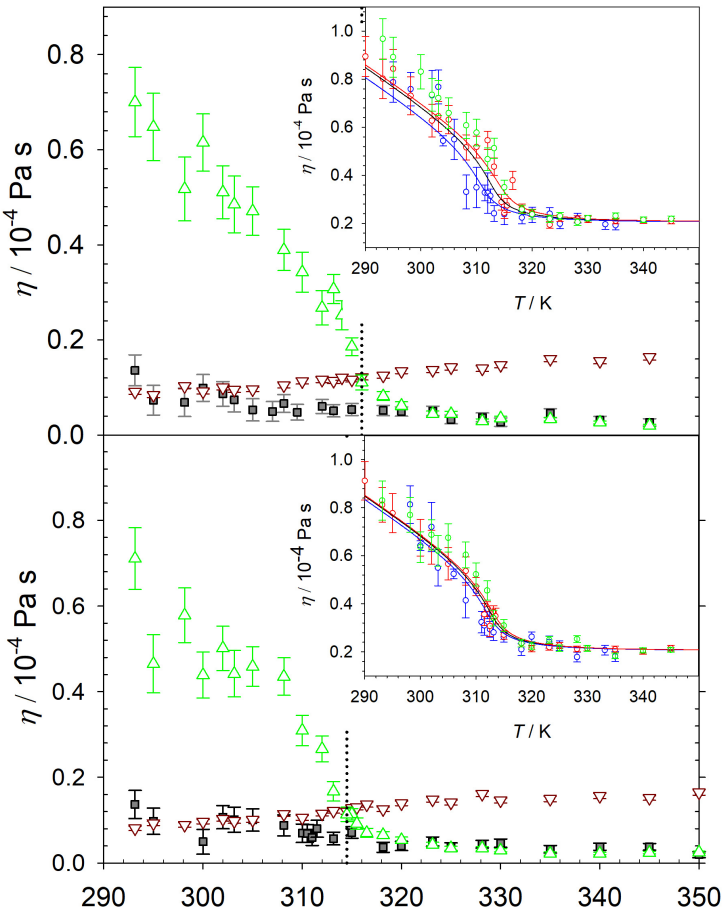

Figure S35: Temperature dependence of the kinetic η_{kk} (brown triangles), configurational η_{cc} (green triangles) and kinetic-configurational η_{kc} (grey squares) contributions to the shear viscosity of $scCO_2$ mixtures with 0.6 (top) and 0.3 mol% (bottom) of naphthalene along the isobar $p = 9$ MPa. The dotted line indicates the Widom line temperature calculated with the criterion of Bell et al.[19]. The inset shows the temperature dependence of the shear viscosity of $scCO_2$ (red) with 0.5 (top) and 1.5 mol% (bottom) of methane (blue), isobutane (red) as well as with 0.3 mol% (bottom) and 0.6 mol% (top) naphthalene (green) along $p = 9$ MPa. In the inset, circles show simulation data and solid lines EOS data. The reference correlation for the shear viscosity by Laesecke et al.[20] was used for pure $scCO_2$. An extended corresponding states approach[21] was used for the mixtures.

Structural properties

Average coordination number

The average coordination number $N_{\text{A-B}}$(r) between like and unlike molecules can be calculated from the integral of the radial distribution function $g_{\text{A-B}}(r)$

$$N_{\text{A-B}}(r) = 4\pi\rho_{\text{B}} \int_0^{r_{\text{min}}} r^2 g_{\text{A-B}}(r) dr, \tag{S5}$$

where r_{min} is the position of the first minimum and ρ_{B} the number density of the site molecular species B.

Microscopic structure of scCO$_2$ mixtures

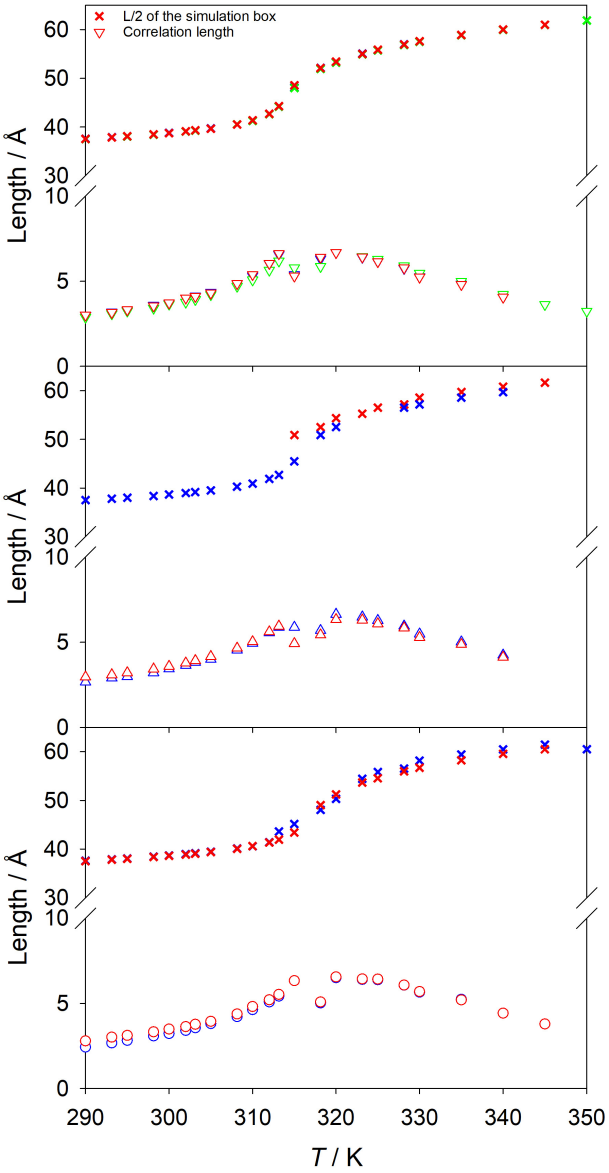

Figure S36: Correlation length (open symbols) and half of the edge length of the cubic simulation volume (crosses) for scCO$_2$ diluted with 0.5 (top), 1.0 (center) and 1.5 mol% (bottom) of benzene (red), toluene (blue) and naphthalene (green) over temperature along the isobar $p = 9$ MPa.

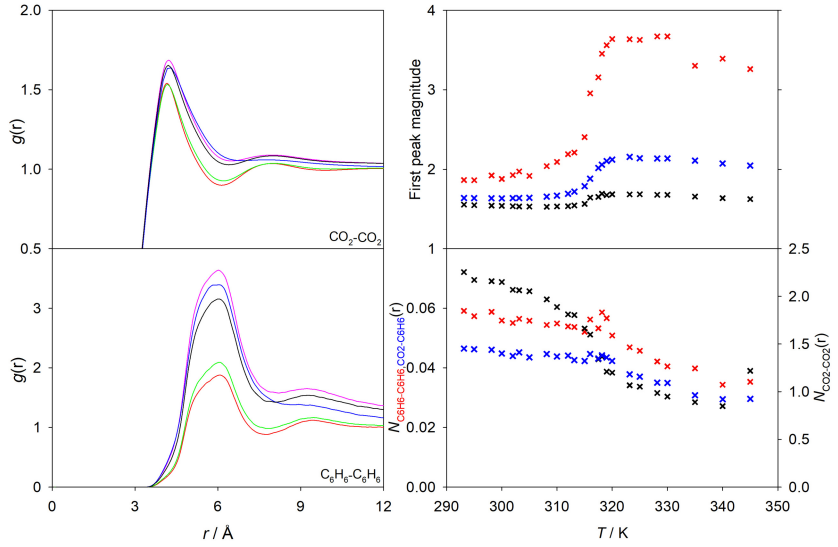

Figure S37: Microscopic structure of the scCO$_2$ mixture with 1.5 mol% of benzene at $p = 9$ MPa. Center-of-mass radial distribution functions $g(r)$ for CO$_2$-CO$_2$ (top left) and C$_6$H$_6$-C$_6$H$_6$ (bottom left) are shown for five temperatures: 300 K (red), 310 K (green), 317.5 K (black), 320 K (pink) and 340 K (blue). The magnitude of the first peak (top right) and the average coordination number (bottom right) for CO$_2$-CO$_2$ (black), C$_6$H$_6$-C$_6$H$_6$ (red) and CO$_2$-C$_6$H$_6$ (blue) as a function of temperature are depicted by crosses.

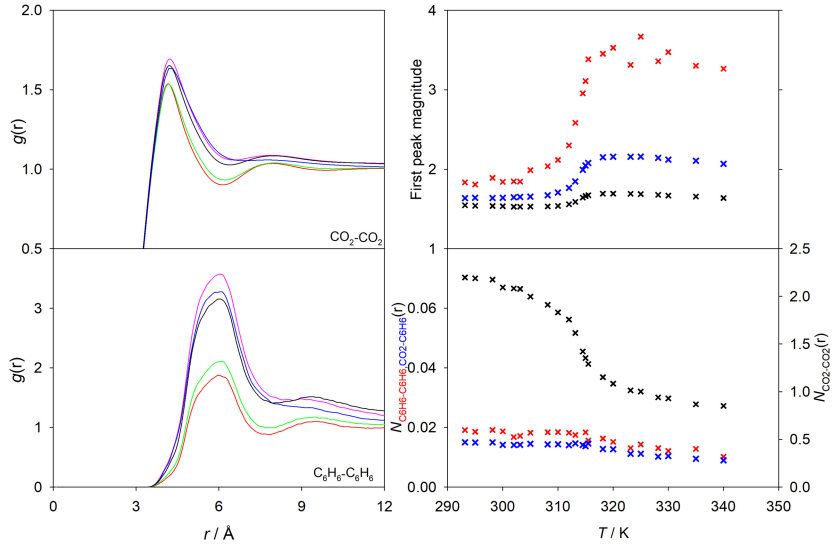

Figure S38: Microscopic structure of the scCO$_2$ mixture with 0.5 mol% of benzene at $p = 9$ MPa. Center-of-mass radial distribution functions $g(r)$ for CO_2-CO_2 (top left) and C_6H_6-C_6H_6 (bottom left) are shown for five temperatures: 300 K (red), 310 K (green), 315.5 K (black), 320 K (pink) and 340 K (blue). The magnitude of the first peak (top right) and the average coordination number (bottom right) for CO_2-CO_2 (black), C_6H_6-C_6H_6 (red) and CO_2-C_6H_6 (blue) as a function of temperature are depicted by crosses.

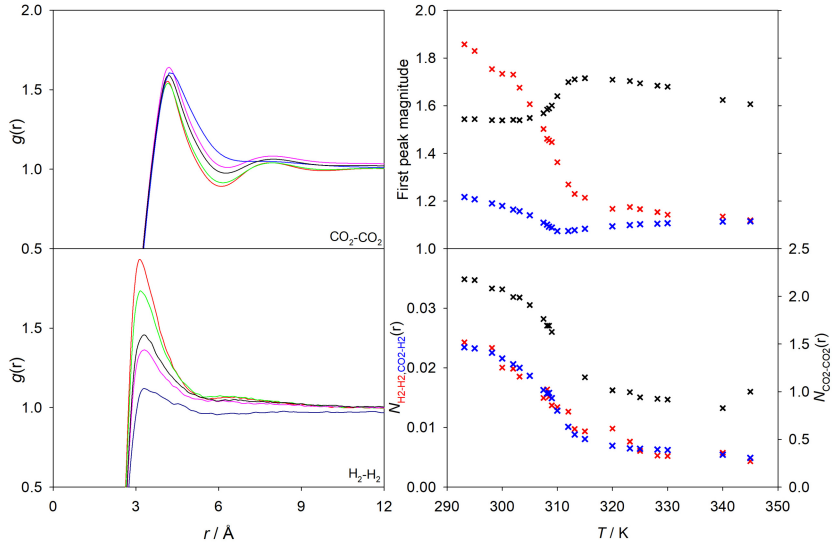

Figure S39: Microscopic structure of the scCO$_2$ mixture with 1.0 mol% of hydrogen at $p = 9$ MPa. Center-of-mass radial distribution functions $g(r)$ for CO$_2$-CO$_2$ (top left) and H$_2$-H$_2$ (bottom left) are shown for five temperatures: 290 K (red), 300 K (green), 308.5 K (black), 310 K (pink) and 340 K (blue). The magnitude of the first peak (top right) and the average coordination number (bottom right) for CO$_2$-CO$_2$ (black), H$_2$-H$_2$ (red) and CO$_2$-H$_2$ (blue) as a function of temperature are depicted by crosses.

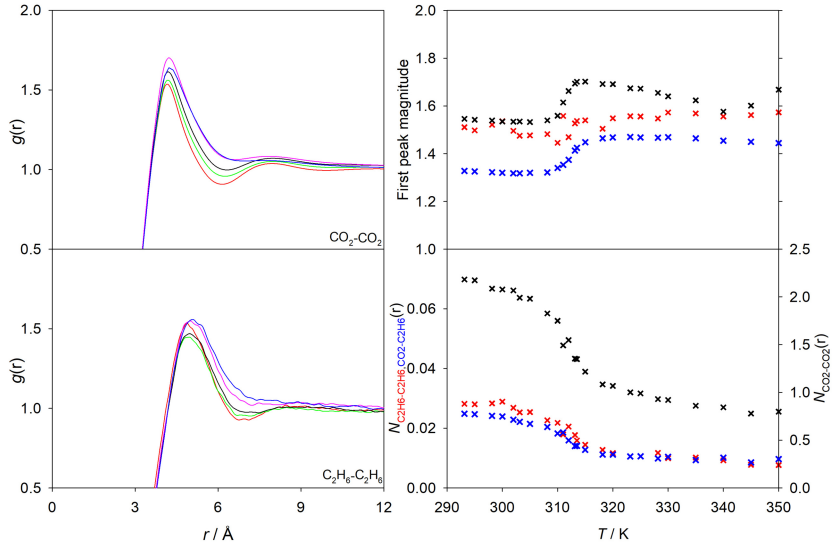

Figure S40: Microscopic structure of the scCO$_2$ mixture with 1.0 mol% of ethane at $p = 9$ MPa. Center-of-mass radial distribution functions $g(r)$ for CO$_2$-CO$_2$ (top left) and C$_2$H$_6$-C$_2$H$_6$ (bottom left) are shown for five temperatures: 300 K (red), 310 K (green), 312 K (black), 320 K (pink) and 340 K (blue). The magnitude of the first peak (top right) and the average coordination number (bottom right) for CO$_2$-CO$_2$ (black), C$_2$H$_6$-C$_2$H$_6$ (red) and CO$_2$-C$_2$H$_6$ (blue) as a function of temperature are depicted by crosses.

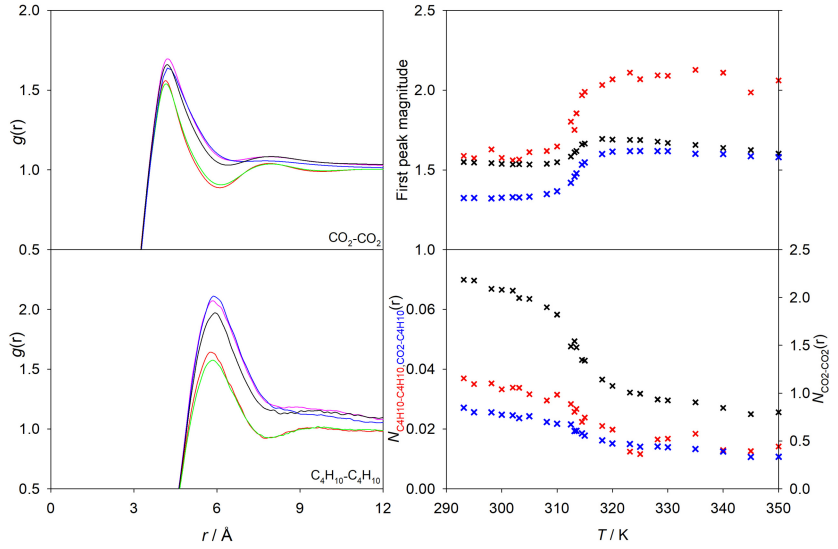

Figure S41: Microscopic structure of the scCO$_2$ mixture with 1.0 mol% of isobutane at $p = 9$ MPa. Center-of-mass radial distribution functions $g(r)$ for CO$_2$-CO$_2$ (top left) and C$_4$H$_{10}$-C$_4$H$_{10}$ (bottom left) are shown for five temperatures: 290 K (red), 300 K (green), 314.5 K (black), 320 K (pink) and 340 K (blue). The magnitude of the first peak (top right) and the average coordination number (bottom right) for CO$_2$-CO$_2$ (black), C$_4$H$_{10}$-C$_4$H$_{10}$ (red) and CO$_2$-C$_4$H$_{10}$ (blue) as a function of temperature are depicted by crosses

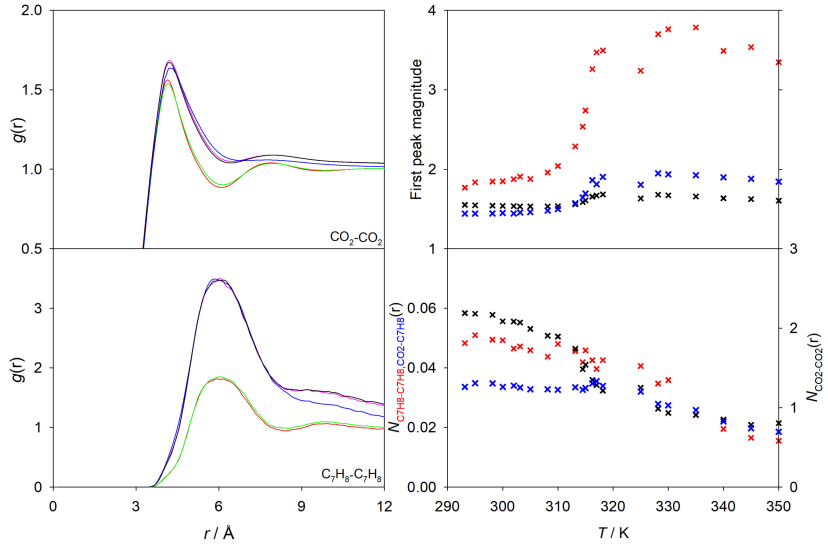

Figure S42: Microscopic structure of the scCO$_2$ mixture with 1.0 mol% of toluene at $p = 9$ MPa. Center-of-mass radial distribution functions $g(r)$ for CO$_2$-CO$_2$ (top left) and C$_7$H$_8$-C$_7$H$_8$ (bottom left) are shown for five temperatures: 290 K (red), 300 K (green), 317 K (black), 320 K (pink) and 340 K (blue). The magnitude of the first peak (top right) and the average coordination number (bottom right) for CO$_2$-CO$_2$ (black), C$_7$H$_8$-C$_7$H$_8$ (red) and CO$_2$-C$_7$H$_8$ (blue) as a function of temperature are depicted by crosses.

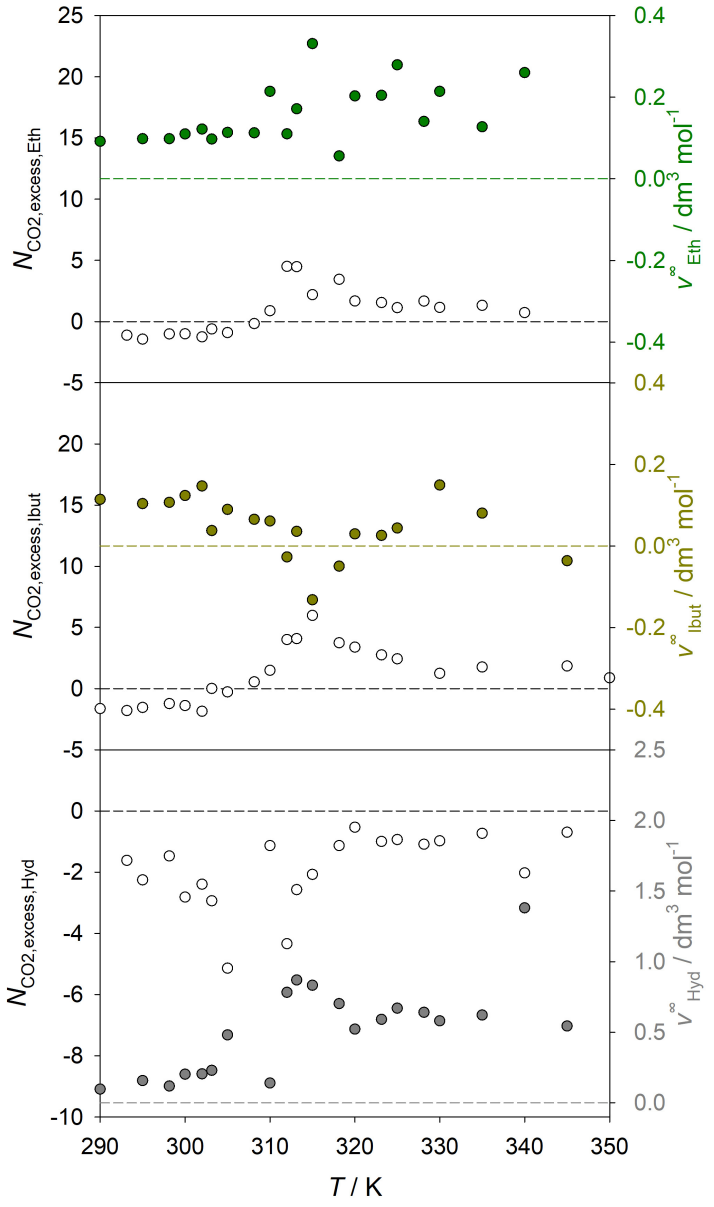

Figure S43: Excess coordination number (open symbols) and partial molar volume of the solute component at infinite dilution (solid symbols) for scCO$_2$ mixed with ethane (top), isobutane (center) and hydrogen (bottom) along the isobar $p = 9$ MPa. Both properties were calculated from Kirkwood-Buff integrals[22] corrected with the procedure by Ganguly and van der Vegt[23]. Dashed lines indicate the zero values of the two vertical axes.

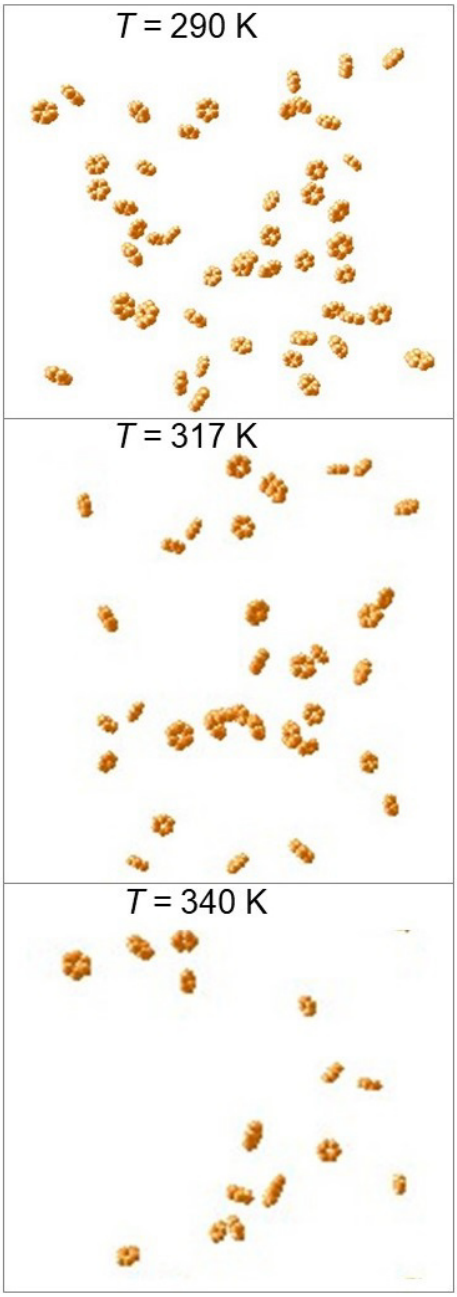

Figure S44: Snapshots of $scCO_2$ (not shown) mixed with 1.0 mol% of benzene at three temperatures: $T = 290$ K (top), 317 K (center) and 340 K (bottom).

References

1. H. C. Andersen, *J. Chem. Phys.*, 1980, **72**, 2384–2393.
2. R. Lustig, *Mol. Phys.*, 1988, **65**, 175–179.
3. H. Flyvbjerg and H. G. Petersen, *J. Chem. Phys.*, 1989, **91**, 461–466.
4. J. Vrabec, Y.-L. Huang and H. Hasse, *Fluid Phase Equilib.*, 2009, **279**, 120–135.
5. S. Stephan, M. T. Horsch, J. Vrabec and H. Hasse, *Mol. Simul.*, 2019, **45**, 806–814.
6. O. Kunz and W. Wagner, *J. Chem. Eng. Data*, 2012, **57**, 3032–3091.
7. C.-H. Kim, P. Vimalchand and M. D. Donohue, *Fluid Phase Equilib.*, 1986, **31**, 299–311.
8. L. A. Weber, *J. Chem. Eng. Data*, 1989, **34**, 171–175.
9. P. Naidoo, D. Ramjugernath and J. D. Raal, *Fluid Phase Equilib.*, 2008, **269**, 104–112.
10. H.-J. Ng and D. B. Robinson, *J. Chem. Eng. Data*, 1978, **23**, 325–327.
11. O. Fandiño, J. M. Trusler and D. Vega-Maza, *Int. J. Greenh. Gas Con.*, 2015, **36**, 78–92.
12. J. Davalos, W. R. Anderson, R. E. Phelps and A. J. Kidnay, *J. Chem. Eng. Data*, 1976, **21**, 81–84.
13. R. A. Harris, M. Wilken, K. Fischer, T. M. Letcher, J. D. Raal and D. Ramjugernath, *Fluid Phase Equilib.*, 2007, **260**, 60–64.
14. I.-C. Yeh and G. Hummer, *J. Phys. Chem. B*, 2004, **108**, 15873–15879.
15. C. J. Leverant, J. A. Harvey and T. M. Alam, *J. Phys. Chem. Lett.*, 2020, **11**, 10375–10381.
16. R. Span and W. Wagner, *J. Phys. Chem. Ref. Data*, 1996, **25**, 1509–1596.

17. E. Lemmon, I. H. Bell, M. Huber and M. McLinden, *NIST Standard Reference Database 23: Reference Fluid Thermodynamic and Transport Properties-REFPROP, Version 10.0, National Institute of Standards and Technology*, 2018, Gaithersburg, Maryland 20899.

18. D. Banuti, *J. Supercrit. Fluids*, 2015, **98**, 12–16.

19. I. H. Bell, S. Delage-Santacreu, H. Hoang and G. Galliero, *J. Phys. Chem. Lett.*, 2021, **12**, 6411–6417.

20. A. Laesecke and C. D. Muzny, *J. Phys. Chem. Ref. Data*, 2017, **46**, 013107.

21. J. C. Chichester and M. L. Huber, *NISTIR 6650: Documentation and assessment of the transport property model for mixtures implemented in NIST REFPROP (Version 8.0)*, US Department of Commerce, National Institute of Standards and Technology, 2008.

22. R. Fingerhut and J. Vrabec, *Fluid Phase Equilib.*, 2019, **485**, 270–281.

23. P. Ganguly and N. F. A. van der Vegt, *J. Chem. Theory Comput.*, 2013, **9**, 1347–1355.